CRREL REPORT 82-39

(12)

US Army Corps of Engineers
Cold Regions Research & Engineering Laboratory

The brine zone in the McMurdo Ice Shelf, Antarctica

For conversion of SI metric units to U.S./ British customary units of measurement consult ASTM Standard E380, Metric Practice Guide, *published by the American Society for Testing and Materials, 1916 Race St., Philadelphia, Pa. 19103.*

Cover: Coring at site of brine step on the McMurdo Ice Shelf in January 1977. Mt. Erebus is seen in the background.

CRREL Report 82-39

December 1982

The brine zone in the McMurdo Ice Shelf, Antarctica

A. Kovacs, A.J. Gow, J.H. Cragin and R.M. Morey

Prepared for
NATIONAL SCIENCE FOUNDATION
Approved for public release; distribution unlimited.

Unclassified

SECURITY CLASSIFICATION OF THIS PAGE (When Data Entered)

REPORT DOCUMENTATION PAGE

READ INSTRUCTIONS BEFORE COMPLETING FORM

1. REPORT NUMBER CRREL Report 82-39	2. GOVT ACCESSION NO. A124516
3. RECIPIENT'S CATALOG NUMBER	
4. TITLE (and Subtitle) THE BRINE ZONE IN THE McMURDO ICE SHELF, ANTARCTICA	5. TYPE OF REPORT & PERIOD COVERED 6. PERFORMING ORG. REPORT NUMBER
7. AUTHOR(s) A. Kovacs, A.J. Gow, J.H. Cragin and R.M. Morey	8. CONTRACT OR GRANT NUMBER(s) NSF-DPP 74-23654 NSF-DPP 8004221
9. PERFORMING ORGANIZATION NAME AND ADDRESS U.S. Army Cold Regions Research and Engineering Laboratory Hanover, New Hampshire 03755	10. PROGRAM ELEMENT, PROJECT, TASK AREA & WORK UNIT NUMBERS
11. CONTROLLING OFFICE NAME AND ADDRESS Division of Polar Programs National Science Foundation Washington, D.C. 20314	12. REPORT DATE December 1982 13. NUMBER OF PAGES 35
14. MONITORING AGENCY NAME & ADDRESS(if different from Controlling Office)	15. SECURITY CLASS. (of this report) Unclassified 15a. DECLASSIFICATION/DOWNGRADING SCHEDULE

16. DISTRIBUTION STATEMENT (of this Report)

Approved for public release; distribution unlimited.

17. DISTRIBUTION STATEMENT (of the abstract entered in Block 20, if different from Report)

18. SUPPLEMENTARY NOTES

19. KEY WORDS (Continue on reverse side if necessary and identify by block number)

Antarctica	Ice shelves
Brines	Radio echo sounding
Firn	
Glaciers	

20. ABSTRACT (Continue on reverse side if necessary and identify by block number)

Observations of a 4.4-m-high brine step in the McMurdo Ice Shelf, Antarctica, show that it has migrated about 1.2 km in 4 years. The present brine wave is overriding an older brine-soaked layer. This migration is proof of the dynamic nature of the step, which is the leading edge of a brine wave that originated at the shelf edge after a major break-out of the McMurdo Ice Shelf. The inland boundary of brine penetration is characterized by a series of descending steps that are believed to represent terminal positions of separate intrusions of brine of similar origin. The inland boundary of brine percolation is probably controlled largely by the depth at which brine encounters the firn/ice transition (43 m). However, this boundary is not fixed by permeability considerations alone, since measurable movement of brine is still

Unclassified

SECURITY CLASSIFICATION OF THIS PAGE (When Data Entered)

20. Abstract (cont'd.)

occurring at the inland boundary. Freeze-fractionation of the seawater as it migrates through the ice shelf preferentially precipitates virtually all sodium sulfate, and concomitant removal of water by freezing in the pore spaces of the infiltrated firn produces residual brines approximately six times more concentrated than the original seawater.

PREFACE

This report was prepared by Austin Kovacs, Research Civil Engineer, of the Applied Research Branch, Experimental Engineering Division, U.S. Army Cold Regions Research and Engineering Laboratory; Dr. Anthony J. Gow, Research Geologist, and James H. Cragin, Research Chemist, of the Snow and Ice Branch, Research Division, CRREL; and Rexford M. Morey, Geophysical Systems Consultant and CRREL Expert, Nashua, N.H.

Funding for this study was provided by the Division of Polar Programs, National Science Foundation, Grant NSF DPP 74-23654 and 8004221.

The assistance of Thomas Fenwick during various field surveys is acknowledged. John D. Palmer of the New Zealand Department of Lands and Survey kindly took triangulation survey data from stations along the inland brine boundary and arranged for their computer analysis and plotting on the McMurdo area map grid. The authors thank *Dr. Samuel C. Colbeck of CRREL for reviewing this report.*

CONTENTS

ILLUSTRATIONS

TABLES

THE BRINE ZONE IN THE MCMURDO ICE SHELF, ANTARCTICA

A. Kovacs, A.J. Gow, J.H. Cragin and R.M. Morey

INTRODUCTION

The occurrence of brine-soaked firn in Antarctic ice shelves has been reported by Dubrovin (1962) for the Lazarev Ice Shelf, Stuart and Bull (1963) for a small ice shelf near Wilkes Station, Smith and Evans (1972) for the Wordie, Brunt and Larsen Ice Shelves, and Thomas (1973) for the Brunt Ice Shelf. This phenomenon, however, is best known for the McMurdo Ice Shelf as reported, for example, by Stuart and Bull (1963), Risk and Hochstein (1967), Heine (1968), Clough (1973), and Kovacs and Gow (1975, 1977b). Several mechanisms have been suggested for the occurrence of brine soaking, including vertical percolation of seawater from the bottom, lateral infiltration from the shelf edge, and upward diffusion along ice crystal boundaries. The most recent work by Kovacs and Gow (1975, 1977b) tends to favor a process of lateral infiltration into dry firn by seawater. Essential to this concept of infiltration of ice shelves by seawater is the need for substantially rapid elimination of excess water by freezing within pore spaces in the permeable firn. This process leads to the formation of concentrated brine capable of remaining liquid at the temperatures encountered in the infiltrated firn. Such a process is also accompanied by changes in brine chemistry (Wilson and Heine 1964, Heine 1968, Cragin et al. 1982) and very substantial isotopic exchange between the brine and the firn (Stewart 1975).

OBJECTIVES

The major objectives of this study were to delineate accurately the terminal (inland) boundary of seawater infiltration in the McMurdo Ice Shelf and to examine the physical structure, chemistry, depth characteristics and lateral continuity of the brine layer. These investigations combined radio echo profiling with core drilling at sites selected on the basis of the radio profiling results. Coring in this manner permitted direct examination of the brine infiltrated and noninfiltrated ice shelf structure. Studies conducted on the cores included chemical analysis of brine-impregnated samples as a means of monitoring the freeze-concentration of the seawater as it permeated the ice shelf firn, density profile measurements, and petrographic examinations of the structure of the brine-infiltrated firn. The ultimate objective was to resolve four questions: 1) What are the principal mechanisms by which seawater infiltrates the McMurdo Ice Shelf? 2) What are the structural relationships of the brine zone to those parts of the ice shelf that remain unaffected by the infiltration of seawater? 3) Why does the infiltration of brine terminate where it does? 4)Is this termination of brine migration mainly controlled by permeability considerations or are other factors involved?

The study was confined to the portion of the Ross Ice Shelf generally designated the McMurdo Ice Shelf (see Fig. 1). The part affected by brine infiltration is included within the area of net sur-

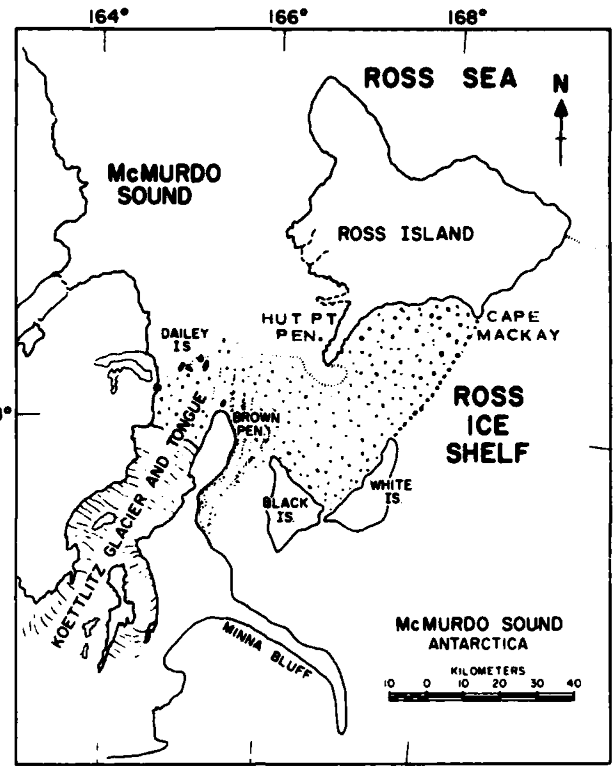

Figure 1. Sketch map of McMurdo Sound and environs showing the portion of the Ross Ice Shelf designated the McMurdo Ice Shelf (dotted area).

face snow accumulation and shelf bottom ablation which occurs mainly in the region directly east and south of Hut Point Peninsula. Further west the ice shelf regime gives way to net surface ablation and bottom freezing.

ANALYTICAL TECHNIQUES

Radio echo profiling

The depth characteristics, lateral continuity and inland boundary of seawater infiltration into the McMurdo Ice Shelf were determined in January 1977 with a dual-antenna radio echo profiling system. The signal information, i.e. the two-way travel time of the transmitted wavelet to and from various reflecting interfaces, was displayed on a graphic recorder and stored on a magnetic tape recorder for later playback and analysis. The dual-antenna arrangement is depicted in Figure 2 and an example of a received waveform is shown in Figure 3. With the dual-antenna arrangement, it was possible to determine the velocity of propagation of the electromagnetic (EM) wave in the firn

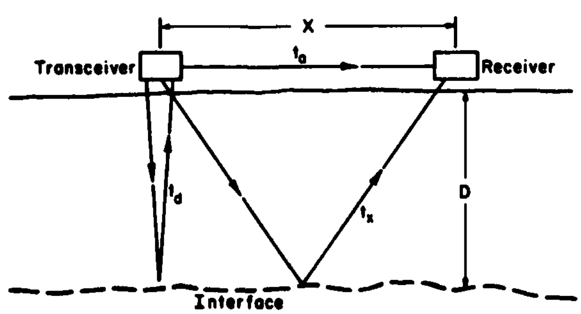

Figure 2. Schematic of dual-antenna configuration and transmitted wavelet paths.

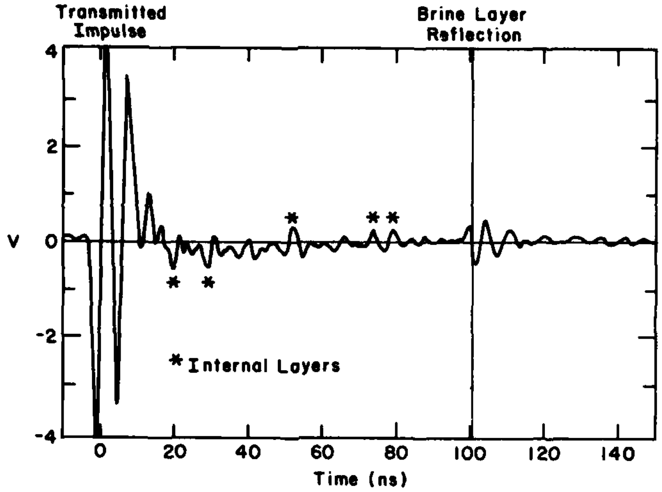

Figure 3. Example of received radio echo wavelet. In the graphic record many horizons or internal layers were observed in the ice shelf firn. These layers could be tracked for many kilometers. Their voltage amplitude signature is shown above.

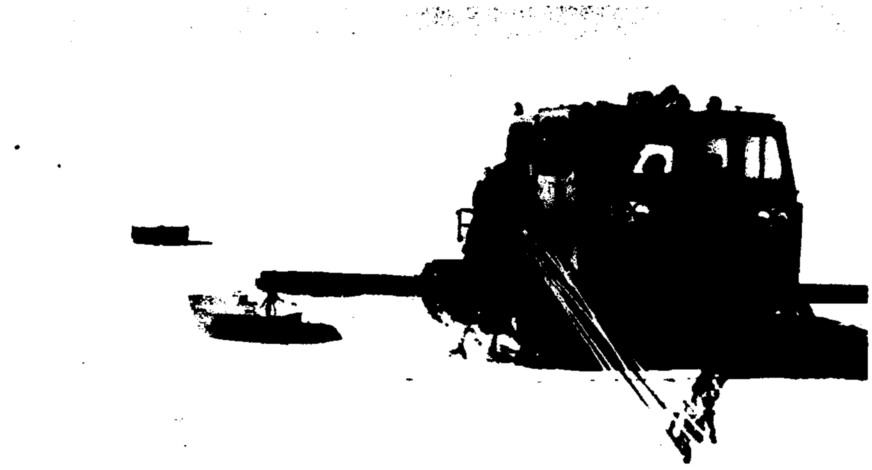

a.

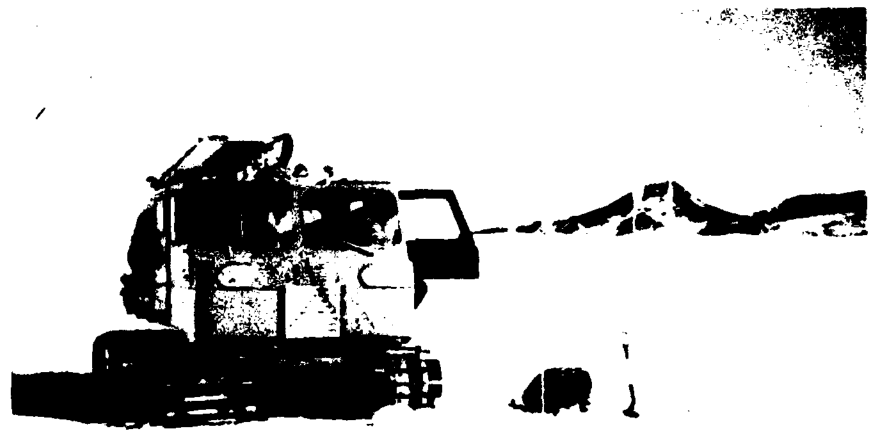

b.

***Figure 4.** Dual antenna radio echo profiling arrangement (a) and snow pit studies at site of 4.4-m-high brine step at station 10 (b).*

and the firn's effective bulk dielectric constant, irrespective of the firn's changing properties due to density.

One antenna operated in a transmit-receive mode and the second in a receive-only mode. The antennas were placed a fixed distance apart on the snow surface and moved as a unit (see Fig. 4). The effective velocity (V_e) of the EM wave was then determined by:

$$V_e = \frac{x}{\sqrt{t_x^2 - t_d^2}} \tag{1}$$

where x = distance between centers of the two antennas

t_d = vertical travel time from transceiver antenna to and from the subsurface interface

t_x = travel time from transceiver antenna to subsurface interface to receive-only antenna ($t_{x'}$) plus time t_a

t_a = air-wave travel time between antennas (see Fig. 2).

A more detailed description of the methodology associated with use of the dual-antenna sounding system can be found in Kovacs and Morey (1979).

With the effective velocity of propagation thus determined, it is then possible to determine brine layer depth D from

$$D = \frac{V_e t_d}{2} \tag{2}$$

and the real effective bulk dielectric constant ϵ_{re} of the firn from

$$\epsilon_{re} = \left|\frac{t_d c}{2D}\right|^2 \tag{3}$$

where c is the free space electromagnetic velocity.

In addition to furnishing a continuous trace of the top of the brine layer the radio echo profiler can also detect such features as internal firn layering, cracks, and relict brine horizons (Kovacs and Gow 1975, 1977a). However, it should be emphasized here that the major discontinuity observed in radio echo profiling records in the McMurdo Ice Shelf is due entirely to a signal return from the top of the brine layer. This situation has been independently confirmed by drilling and coring at seven locations on the McMurdo Ice Shelf. In all our drill holes we never encountered rock debris or any other englacial material capable of creating such a strong reflecting horizon with the ice shelf.

Core drilling

Drill holes were all located along the line of the main radio echo profiling traverse of January 1977. An electromechanical drill (Fig. 5), designed by Rand (1976) and operated by a team of drillers from the Polar Ice Coring Office (PICO), was used for deep coring at four sites. Three of these holes penetrated the brine layer for distances of up to 2.5 m, but none were drilled deep enough to penetrate the entire brine zone. The fourth and deepest hole was purposely drilled a few meters beyond the brine terminus, as determined by radio echo profiling, so as not to intercept the brine zone. Cores from all four holes were logged and measured on-site for temperature. Those cores infiltrated with brine were cut into ≈10-cm lengths and placed in sealed containers. Cores and samples were then transported back to refrigerated facilities at McMurdo Station, where the brine-soaked samples were first measured and weighed for density determination and then melted. The salinity of the meltwater from each sample was then measured and specimens of the liquid bottled

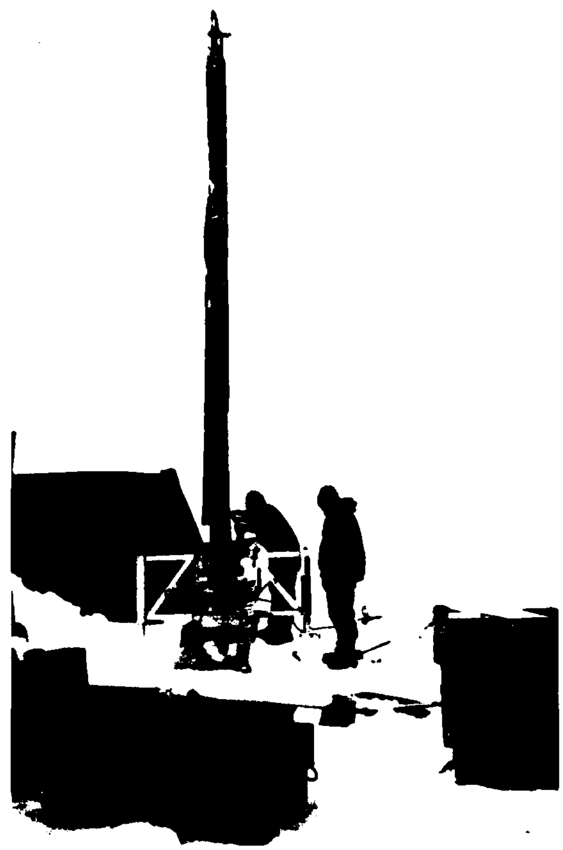

Figure 5. Electromechanical drill hoist assembly used for coring into the ice shelf.

and carefully sealed for subsequent chemical analysis at CRREL. Thin sections of selected samples were also prepared and examined cursorily for crystal/air bubble/brine inclusion relationships. Unfortunately all these sections, together with the remaining brine-soaked samples set aside for additional structural studies, were lost when the McMurdo Station coldroom in which they were stored was accidentally defrosted. Cores from several shallow holes located near the front of the McMurdo Ice Shelf were also investigated in conjunction with cores from the deeper holes. Unused cores were returned to CRREL for archiving and additional analysis.

RESULTS AND DISCUSSION

Brine infiltration survey

During January 1977 radar profiling of the top of the brine layer was conducted along several separate traverses, including the main profile line, which was flagged and resurveyed in November 1978 and January 1981. The main profile line extended from the ice shelf edge to the inland boundary of brine infiltration and for some distance beyond. In addition, the inland boundary of brine infiltration was profiled in detail between Hut Point Peninsula and White Island (Fig. 6). Stations along the boundary were fixed by tri-

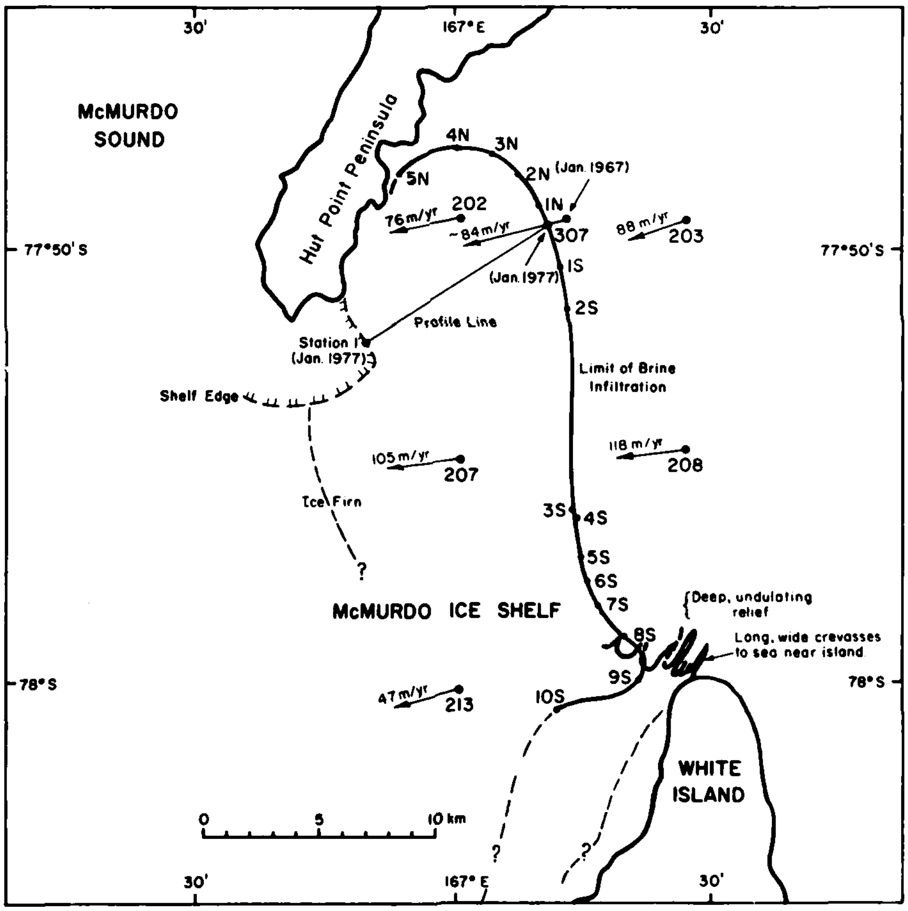

Figure 6. Area encompassed by radio echo profiling surveys. The route of the major profiling traverse and the boundary marking the inland limit of brine infiltration are indicated, together with pertinent data on ice shelf movement and surface features. The boundary marking the westward limit of brine infiltration (the equilibrium line) is also indicated. The shelf to the west of this boundary is ablating glacial ice. The area inside the first dashed line immediately west of White Island is composed of snow ice up to 15 m thick. Snow depth is less than 2.5 m.

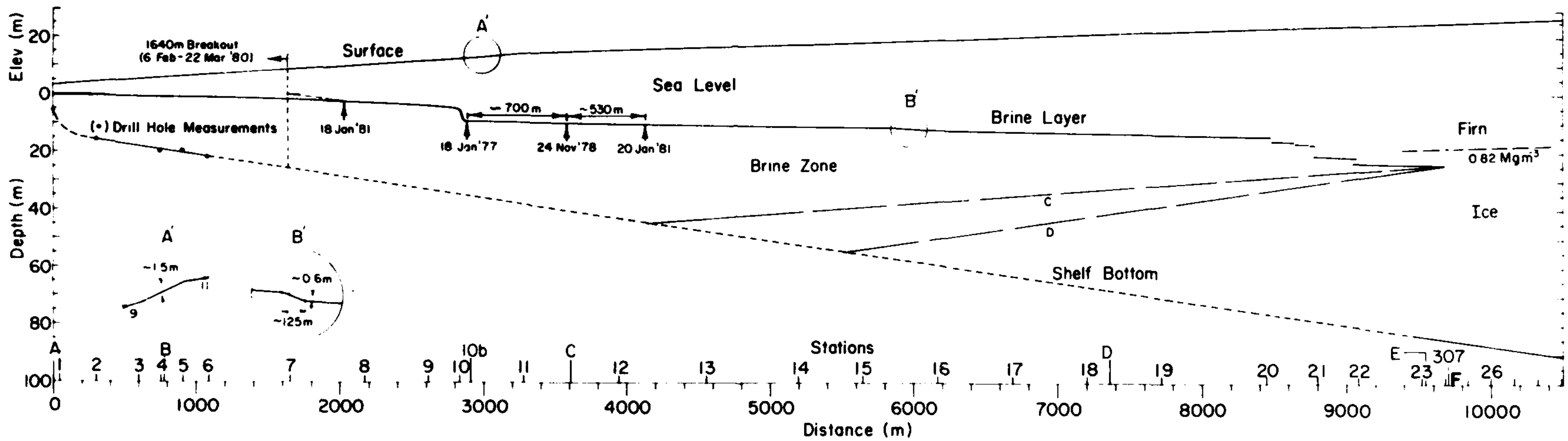

Figure 7. Cross section of the McMurdo Ice Shelf in 1977 along the main radio echo profiling line. Stuart and Bull (1963) first showed the shelf to be wedge-shaped. The location and height of the shelf edge vary in time and space and are functions of shelf movement rates, break-out dates, and the magnitude and rate of melting across the bottom of the ice shelf. Drill hole sites are designated A to F.

Table 1. 1977 McMurdo Ice Shelf station data along traverse from ice front to beyond ice-shelf movement marker 307.

Station no.	*Distance inland (m)*	*Freeboard F (m)*	*Brine depth (m)*	*Brine elevation (−m)*	*Keel depth K (m)*	*Real effective dielectric constant* ϵ_{re}	*Effective EM wave velocity* V_e *(m/ns)*
1	40	3.9	4.7	0.8	—	1.81**	0.223
2	305	4.8	—	—	15.5*	—	—
3	600	5.0	6.0	1.0	—	1.91	0.217
4	750	5.6	—	—	20.0*	—	—
5	910	6.0	—	—	19.5*	—	—
6	1,080	6.5	7.8	1.3	21.5*	1.95	0.225
7	1,640	8.1	10.2	2.1	—	1.99	0.212
8	2,160	10.2	12.8	2.6	—	2.04	0.210
9	2,620	11.6	15.5	3.9	—	2.09	0.208
10	2,840	12.5	16.9	4.4	—	2.10	0.207
10b	2,900	12.7	21.5	8.8	—	2.18	0.203
11	3,280	14.4	23.6	9.2	—	2.18	0.203
12	3,940	15.6	25.4	9.8	—	2.22	0.201
13	4,550	16.7	26.7	10.0	—	2.25	0.200
14	5,190	17.6	27.9	10.3	—	2.29	0.198
15	5,640	18.2	29.2	11.0	—	2.32	0.197
16	6,160	19.4	31.2	11.8	—	2.33	0.196
17	6,680	20.1	32.6	12.5	—	2.34	0.196
18	7,200	20.8	33.8	13.0	—	2.35	0.196
19	7,720	21.7	35.3	13.6	—	2.36	0.195
20	8,480	23.0	37.9	14.9	—	2.43	0.192
21 high	8,800	23.4	40.6	17.2	—	2.46	0.191
21 low	8,800	23.4	44.5	21.1	—	2.50	0.190
22 high	9,080	23.8	45.5	21.7	—	2.49	0.190
22 low	9,080	23.8	47.5	23.7	—	2.52	0.198
23	9,520	24.6	—	—	84.6†	—	—
24	9,660	25.0	49.1	24.1	88.0†	2.52	0.198
307	9,700	25.0	—	—	—	—	—
25	9,840	25.2	—	—	89.7†	—	—
26	10,000	25.4	—	—	90.0†	—	—
27	10,160	25.6	—	—	91.4†	—	—
28	10,320	25.9	—	—	92.4†	—	—
29	10,490	26.2	—	—	93.6†	—	—

* Drill-hole measurements.

† Based on wavelet two-way travel time from snow surface to shelf bottom minus two-way travel time from snow surface to brine elevation at station 24. The ice below brine termination elevation was assumed to have $\epsilon = 2.95$ and therefore $V_e = 0.175$ m/ns.

** Between surface and brine layer.

Note: Brine elevation is distance from sea level to top of brine layer. Keel depth is draft of ice shelf.

angulation survey. The resulting data were computer-analyzed for accurate plotting on the New Zealand survey grid of the area. The northern limit of this brine layer was originally delineated by Clough and Bentley (1967) and Clough (1973), who emplaced bamboo pole markers at intervals along the boundary. In November 1973, new bamboo poles were placed at intervals along the boundary (John Clough, pers. comm.). The 18 January 1977 resurvey of the existing markers 2S, 1S, 1N, 2N, 3N and 4N (Fig. 6) indicated that the brine terminus had moved inland 197, 129, 73, 55, 10 and 9 m beyond these stations respectively during the intervening 3 years, i.e. at average rates of 0.168, 0.110, 0.062, 0.047, 0.009 and 0.008 m/day. The magnitude of brine migration at the first four markers demonstrates that brine infiltration there is still very active. However, the very small movement recorded at markers 3N and 4N would indicate that the brine there is now infiltrating firn with very limited permeability.

The brine layer depth and the effective velocity of propagation of the EM wave and real effective dielectric constant values for the firn, as determined from the ratio echo profile data, versus distance along the main profile line shown in Figure 6 are listed in Table 1. Also listed are the surface elevations (freeboards) determined by topographic survey and the ice shelf keel depths determined by direct drill hole measurement. These data allowed the construction of a representative cross section of the McMurdo Ice Shelf along our main profile line (Fig. 7).

Brine layer steps

Among several important features shown in Figure 7 are a large 4.4-m step in the brine layer located near station 10 and a series of descending steps characterizing the inland termination of the brine layer. These same features, as they appear on the graphic recorder, are illustrated in Figures 8 and 9.

The position of the 4.4-m step in the brine layer, as first observed on 18 January 1977, was carefully flagged and reprofiled on 24 November 1978 (Fig. 7) and again on 20 January 1981. Between 18 January 1977 and 24 November 1978 this step was found to have moved inland about 700 m, equivalent to an average rate of advance of about 1.04 m/day. Between 24 November 1978 and 20 January 1981 the brine step had migrated an additional 530 m inland at an average rate of 0.67 m/day. These measurements of the actual migration of the brine step demonstrated for the first time the dynamic wave-like nature of seawater infiltration within the McMurdo Ice Shelf. This particular brine step almost certainly represents the leading edge of a wave of seawater that entered at the ice front during a recent major break-out of ice in McMurdo Sound. In addition, it would appear that over the 4-year duration of the measurements, brine infiltration has slowed appreciably, most probably in response to a decrease in firn permeability as the brine moved into deeper and denser parts of the ice shelf.

Results of drilling at stations 10 and 10b on either side of the brine step clearly show that the 4.4-m-high brine wave is currently riding on top of an earlier brine-soaked layer. This layer also terminates in a step, some distance inland, and it, together with several other steps located near the present boundary of brine infiltration, are also believed to represent earlier episodes of wave-like intrusions of seawater originating at the ice front. All such intrusions of seawater are believed to be triggered by periodic break-outs of the ice shelf. Through this process firn at the shelf edge in a zone between sea level and the top of the old brine horizon, now located below sea level, becomes exposed to the sea and a new wave of seawater begins to percolate into the ice shelf. This sequence of events is illustrated in Figure 10. From the measured slope of the brine-soaked firn layer, it was estimated that approximately 3 km of the ice shelf had to have broken off to allow for the formation of the 4.4-m-high brine step. Paige (1971) reports that "the most extensive observed periods of ice shelf breakout occurred in February of 1964 and 1965." Approximately 1500 m of shelf calved during these events. Further calving occurred in 1966, 1967, 1968, and apparently in 1970 but these were less extensive. Nevertheless, the sum total of the 1964 through 1970 break-outs must have been about 3 km. Since no brine step record of these events was observed in the radio echo profiles we can only assume that these steps were removed by subsequent break-outs. If ice shelf break-out occurred in February 1970 and the resultant brine wave coincided with the 4.4-m step located 2850 m in from the shelf edge as of January 1977, then the

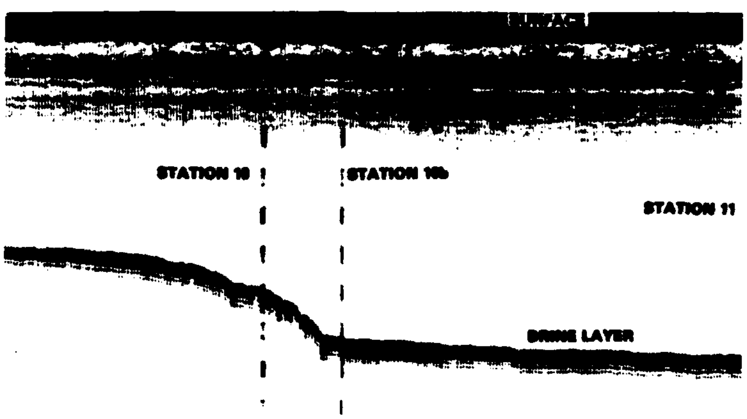

Figure 8. Graphic record of 1977 radio echo data showing the 4.4-m-high brine step located at station 10.

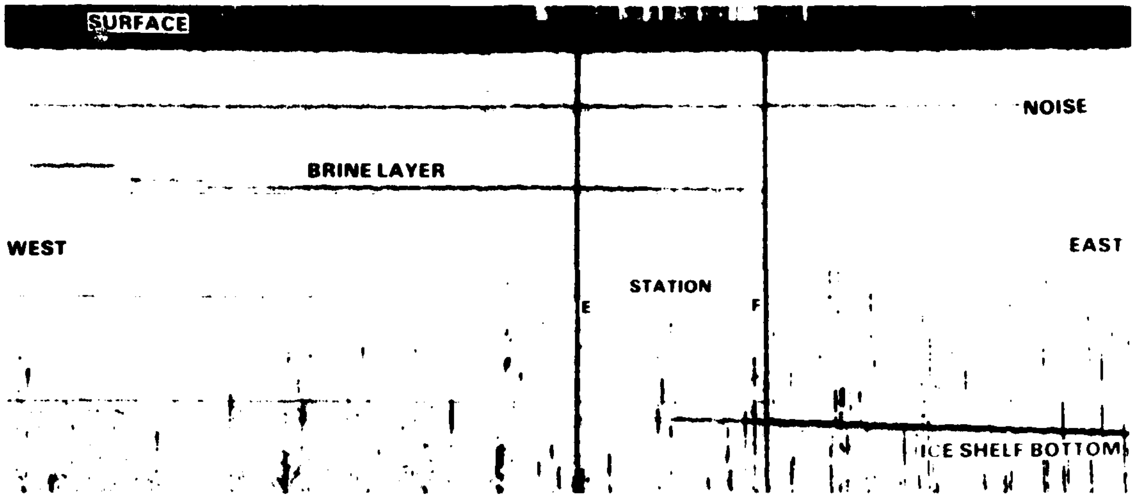

a. Time between horizontal scan lines is about 325 ns and the distance between station E and F is ≈ 200 m.

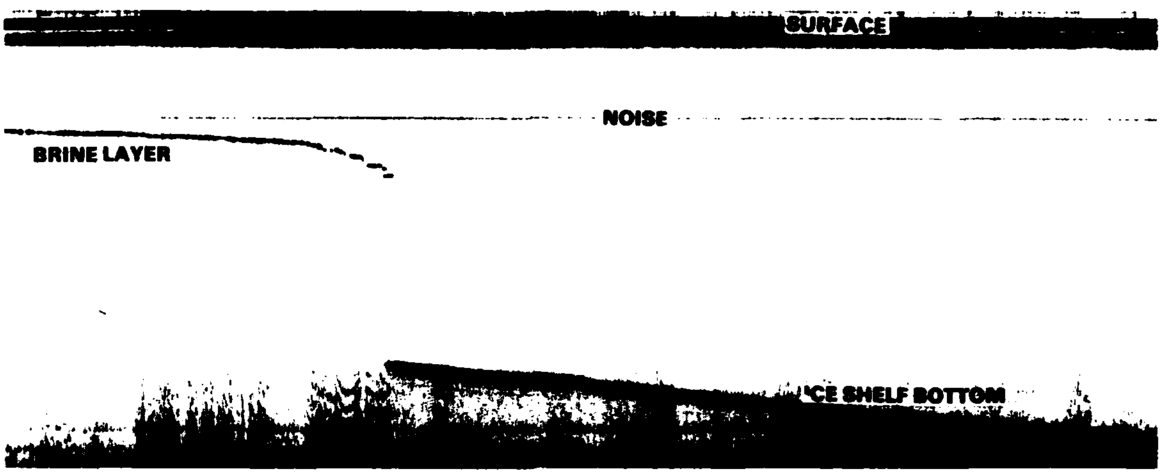

b. 12.0 km of the ice shelf bottom is shown, which reveals a relatively smoothly sloping surface.

Figure 9. Graphic record of 1977 radio echo data showing the stepped nature of several brine layers located near the inland boundary of brine penetration. The fact that the shelf bottom could be observed under the lowest brine layer indicates that the layer is "thin" (2–3 m or less) and/or low loss with respect to electromagnetic energy transmission; otherwise the bottom radio echo would not have been observed. .

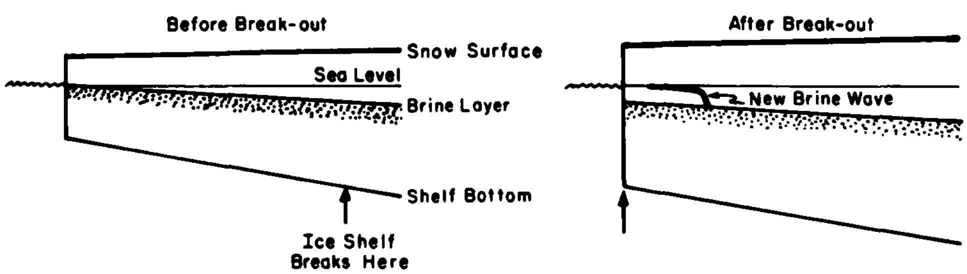

Figure 10. Schematic of ice shelf break-out event leading to formation of new zone of brine-infiltrated firn.

average infiltration velocity of the brine wave would have been about 1.2 m/day. This rate of infiltration is compatible with the value of 1.04 m/day obtained by direct measurement of the 4.4-m step between 18 January 1977 and 24 November 1978.

It was learned from a discussion with Mr. Cass Roper, who was at the New Zealand Scott Base at the time, that between 6 February and 22 March 1980, large sections of the McMurdo Ice Shelf broke off. During one period, the shelf was observed moving vertically 3 to 5 cm at an inland crack. A resurvey of the main profile line in January 1981 revealed that 1640 m of the shelf was then missing. Based upon old records (Heine 1963, Paige 1971) this break-out was one of the largest ever recorded. A new brine layer horizon was detected, situated approximately 1.4 m above the old horizon at the shelf edge and extending inland 375 m, as shown in Figure 7. This infiltration occurred over a period of about 302 days, equivalent to an average rate of brine migration of 1.24 m/day.

Brine infiltration characteristics

Risk and Hochstein (1967) attribute the formation of brine-soaked firn in the McMurdo Ice Shelf to lateral percolation of seawater from the shelf edge. They also embrace the idea of Stuart and Bull (1963), who suggest that vertical brine infiltration occurs through low density bottom firn. However, Risk and Hochstein limited the area where the latter mechanism occurs to a zone extending about 0.5 km in from the shelf edge where permeable firn was considered to be exposed due to bottom melting. If vertical infiltration is occurring in a zone near the shelf edge, one would expect the top of the brine-soaked firn in this area to be in near-hydrostatic equilibrium with the seawater. From our radio echo profile surveys, it was observed that the top of the brine layer, beginning at the very edge of the ice shelf, slopes down below sea level, that is, has a negative gradient. It therefore appears that permeable firn does not now exist on the bottom of the ice shelf. In-situ freezing of water derived from the brine as it laterally infiltrates the firn has effectively blocked off interconnected pores, preventing any upward migration of seawater.

It is interesting to note that Thomas (1975) estimated a brine infiltration rate of 1.10 m/day for the Brunt Ice Shelf, where the firn density (0.570 Mg/m^3), temperature (-10°C) and pressure gradient (1 in 525) were more favorable to seawater infiltration than for the McMurdo Ice Shelf. We can calculate a brine flow velocity u at station 10 following the procedure of Thomas, where

$$u = \frac{B_0}{\eta} \frac{\partial p}{\partial x} \tag{4}$$

and B_0 is the specific permeability of the firn, η is the dynamic viscosity of the brine fluid, and $\partial p / \partial x$ is the pressure gradient of the brine layer. Thomas modified Shimizu's (1970) formula $B_0 = 0.077 \times d^2 \exp(-7.4 \varrho_s)$, where d is the grain diameter and ϱ_s is the density of snow, and has suggested that $B_0 = 9 \times 10^{-4}\ d^2$. We estimated the grain diameter to be 2 mm for 0.7-Mg/m^3 density firn at station 10. The firn temperature was ≈ -14°C and η for the brine at this temperature is $\approx 4.5 \times 10^{-3}$ Pa/s. The hydraulic head, over a distance of 2580 m from station 1 to station 9, is 3.1 m. From eq 4 we calculate a flow velocity of 9.68×10^{-6} m/s or $\approx$ 0.84 m/day. This value fits nicely between the 18 January 1977–24 November 1978 average brine velocity of 1.04 m/day which existed before the brine wave reached station 10, and the 24 November 1978–20 January 1981 average velocity of 0.67 m/day measured after the wave passed station 10.

Core data obtained in November 1978 from holes drilled at stations E and F, on either side of the brine terminus, revealed that "impermeable" firn of density 0.82–0.83 Mg/m^3 (ice by definition) is encountered at a depth of about 43 m, or 6 to 7 m *above* the brine layer at the station E hole, which was located about 120 m inside the brine terminus as measured in January 1977. The hole at station F was located about 77 m beyond the brine terminus, as it existed in January 1977, and no brine was encountered in this 59-m-deep hole when it was drilled in November 1978. From these observations, it might appear that the inland limit of brine infiltration in the McMurdo Ice Shelf is controlled mainly by the depth at which brine encounters the firn/ice transition. At this boundary ice containing liquid brine inclusions is presumably carried downward into the ice shelf and further densified as snow continues to accumulate on the ice shelf surface.

Some estimate of the time that has elapsed since the brine became "locked in" can be obtained from accumulation data reported by Heine (1967), which show that snow accumulation in the vicinity of the brine terminus should average around 25 cm water annually. At station E, where the top of the brine layer is now located 6 to 7 m below the firn/ice transition, we calculate, on the basis of our core density measurements, that the infiltration of brine should have effectively ceased 20 to

25 years ago. However, more recent, very careful profiling of this boundary has revealed that a small but detectable migration of brine is still occurring, apparently by some mechanisms not directly related to firn permeability. Once "locked in," the brine must, with time, descend into deeper and warmer ice. In doing so, the concentrated brine would need to dissolve ice to maintain a brine solution concentration in equilibrium with the in-situ temperature, and this may have contributed to the continued slow inland percolation of the brine.

The slope of the brine layer measured 1 in 832 from the shelf edge to station 9. From station 11 to station 20 the brine layer slope was 1 in 910, and from stations 22 to 24 it had decreased to approximately 1 in 1500. The surface of the ice shelf beyond station 11 sloped approximately 1 in 606, while the bottom of the ice shelf had a slope of about 1 in 137.

If the brine layer along the main profile were to maintain a slope of 1 in 830 beyond station 9 and could move instantly inland to intersect the "impermeable" 0.82-Mg/m^3-density firn/ice transition horizon, it would do so at a maximum distance of about 14 km inland from the 1977 shelf edge. However, this is not likely to occur under existing infiltration conditions because as the brine moves inland it will encounter denser and therefore less permeable firn as well as lower temperatures. These effects will slow the brine infiltration rate and probably limit its inland penetration in the area of our profile to less than 11 km.

A rate of bottom melting of the order of 0.9 to 1.2 m of ice per year has been estimated for stations 202 and 207 (see Fig. 6) by Risk and Hochstein (1967). By assuming an ice bottom ablation rate of 0.9 m/yr it would take some 69 years before the brine-infiltrated firn at station 24 becomes exposed to the sea. Similarly, if bottom melting were occurring at 1.2 m/yr it would take only 52 years for the brine-infiltrated firn to reach the bottom of the ice shelf.

Typical ice shelf movement rates are shown in Figure 6. These rates are taken from Heine (1967) except for that of station 307, which was obtained from the 1972–73 to 1978–79 austral summer survey data on file at the New Zealand Scott Base, Ross Island, Antarctica. In 1978–79, station 307 was moving westward at 84 m/yr. The survey data also indicate that the ice movement at this station is slowing down. If it is assumed that the ice shelf movement in the area of station 307 remains constant at about 80 m/yr during the next 50 to 70 years, and that the ice shelf cross section depicted in Figure 7 remains unchanged, then it is possible to make an approximation of the general area of ice shelf composed of brine-soaked firn and saline ice. At a forward movement of 80 m/yr and a bottom ablation rate of 0.9 m/yr, we estimate that the saline ice near station 307 would reach the bottom of the shelf some 5520 m ahead of its present position and would have moved downward along path C, as shown in Figure 7. Similarly, if the bottom ablation rate were increased to 1.2 m/yr, then the brine-infiltrated ice would move forward some 4160 m along path D before reaching shelf bottom. Path D intersects the firn/ice transition depth at a distance of approximately 10,700 m inland on the cross section. If path C were similarly extended, it would intersect the firn/ice transition at a distance of about 15 km inland. From earlier considerations, this latter distance would appear excessive, suggesting that ice shelf bottom melting is occurring at a rate closer to 1.2 m/yr rather than 0.9 m/yr in the immediate area of the cross section. This would be in keeping with measurements by Paige (1969), who determined from ice movement records and drill hole measurements a shelf-thinning rate of 1.06 m/yr, which when combined with the annual surface accumulation of 0.27 m/yr would require a total bottom melting of 1.33 m/yr for an area located about 0.5 km south of the southern end of our profile line. This ablation rate was subsequently confirmed by Hoffman (1974).

Brine infiltration mechanisms at inland boundary

The above analysis does not consider vertical brine migration, either by diffusion of brine along crystal boundaries (see Eide and Martin 1975), or by intergranular vein flow as described by Nye and Frank (1973) and Raymond and Harrison (1975). As noted earlier, it was thought that brine is unlikely to infiltrate much beyond the firn/ice transition because of lack of permeable pore space. However, between 18 January 1977 and 24 November 1978 the brine terminus was found to have migrated 27.5 m closer to station 307, at an average rate of 0.041 m/day. From 24 November 1978 to 20 January 1981 the terminus had moved an additional 30.5 m to a point 18 m beyond station 307, at an average rate of 0.039 m/day. If this rate was maintained then the brine could be expected to intersect drill hole F (located 37 m beyond station 307) sometime during May or June 1982. Core data from drill station E revealed that the brine was migrating within ice with a density of 0.85 Mg/m^3 and a temperature of -16 °C.

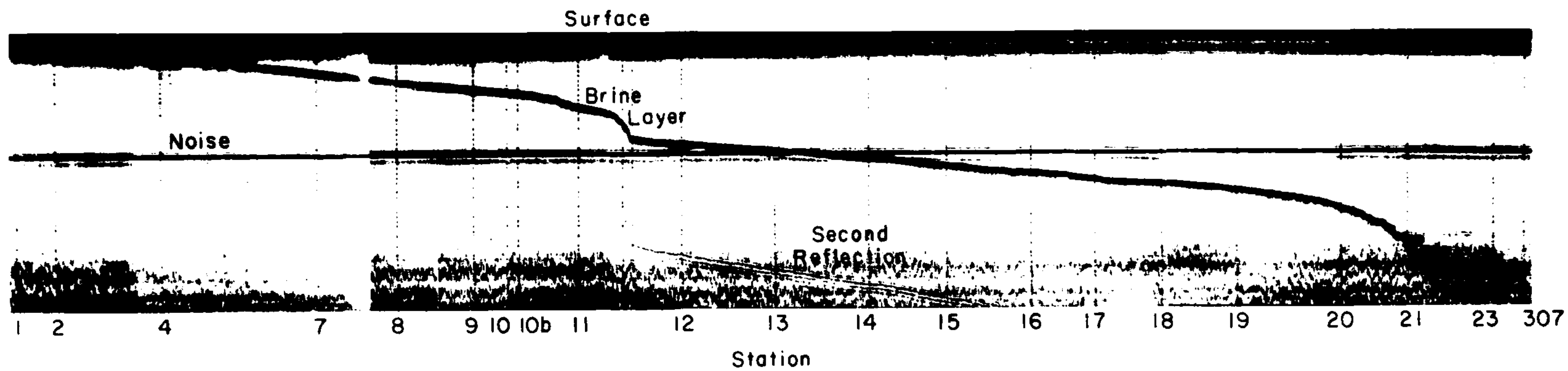

a. The entire radio echo profile along the main traverse line.

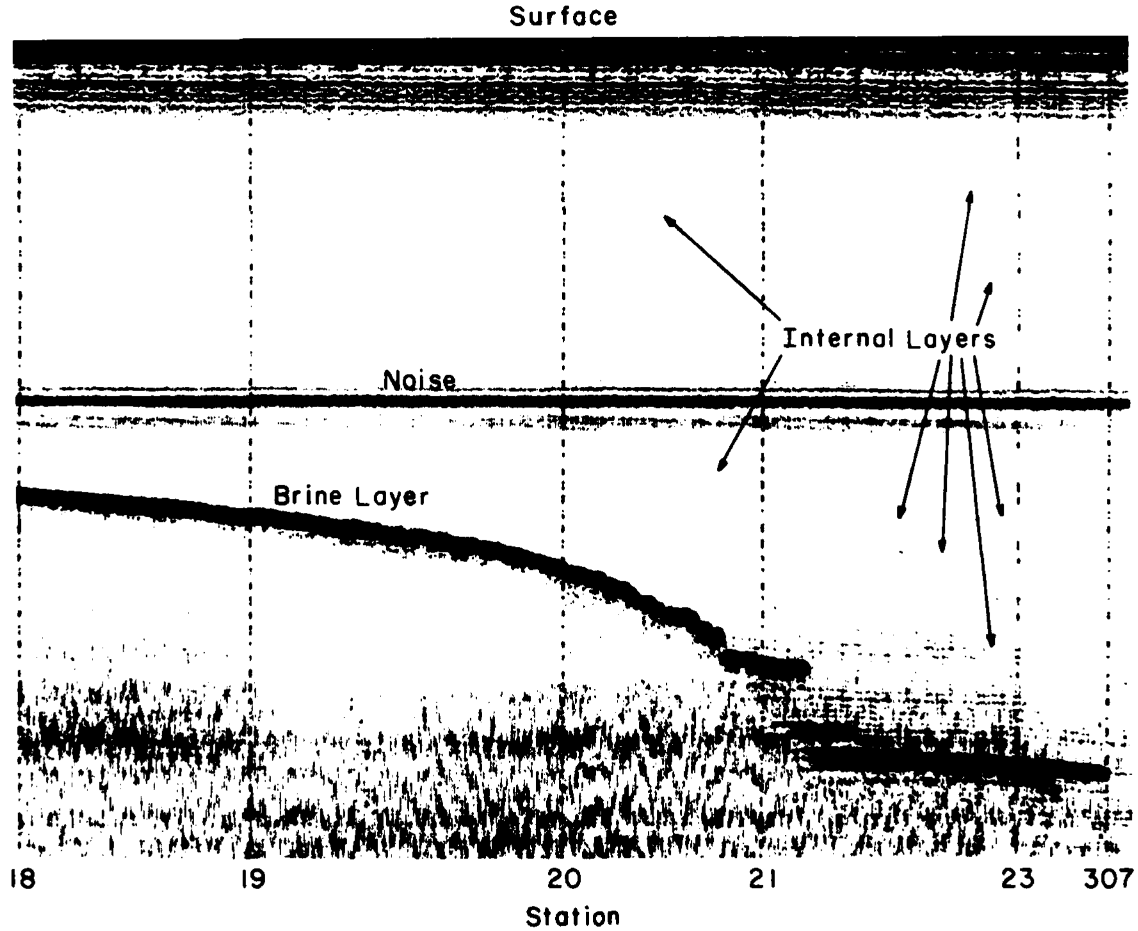

b. The attitude of the brine layer, changing to conform with the firn layering as it approaches the terminus of brine infiltration.

Figure 11. Graphic record of 24 November 1978.

The observed brine velocity of 0.04 m/day is at least three orders of magnitude greater than simple diffusion theory (through the ice lattice) would predict (see, for example, Hoekstra et al. 1965 and Seidensticker 1966). Ice with a density of 0.85 Mg/m^3 would be permeable to brine only in the presence of intergranular veins such as exist in ice in temperate glaciers. However, such intergranular connections are not likely to exist in ice at temperatures of −16°C. One possible explanation of continued migration of the brine is the dissolution of ice by the concentrated brine as it is transported into deeper and warmer parts of the ice shelf through the process of surface snow accumulation and bottom ice ablation deflecting the ice shelf downward. However, considering the magnitude of the movement, in relation to the small change in temperature encountered by the brine, it is unlikely that this mechanism alone could account for the observed rate of lateral brine migration. Preliminary field observations of thin sections of brine-soaked ice showed the brine to be located in bubble-like vesicles. Unfortunately, an accidental defrosting of the McMurdo Station coldroom destroyed all the samples before detailed investigations of the degree of interconnectivity of vesicles and air bubbles in the brine-soaked ice could be completed.

An interesting fact that may be related to a change in the mechanism of brine migration was the change observed in the attitude of the brine layer as it passed through the region of the firn/ice transition (Fig. 11). An inspection of Figure 11 shows that prior to reaching the firn/ice transition, the top of the brine layer cuts obliquely across the firn layering. However, just beyond the transition the top of the brine layer changes attitude to conform with the stratification and this situation continues to the brine terminus.

Confirmation of brine depths by drilling

The calculated depth of the brine layer, as determined from the 1977 radio echo data, was verified by direct measurement in several drill holes that penetrated the top of the brine layer. For example, using the January 1977 radio echo data we calculated a depth of 49 m to the brine layer at drilling station E, located 9560 m in from the shelf edge. Coring in December 1978 revealed a depth of 50.4 m. During the preceding two winters about 0.9 m of new snow had accumulated. Adding this accumulation to the 49-m depth gives a difference between the calculated and measured brine depths of 0.5 m, or less than 1%. Drilling was also undertaken in 1974 and 1977. This drilling included three holes (B, 10 and 10b) from which cores were obtained to a maximum depth of 22.5 m, and four other holes that were drilled to the bottom of the ice shelf to measure ice shelf thickness. The four core holes drilled in 1978 and designated stations C, D, E and F in Figure 7 were originally located 3590, 7370, 9560 and 9700 m respectively in from the shelf edge. The first three holes (C–E) encountered the brine layer at depths of 19.4, 33.8 and 50.4 m, respectively. The brine layer was located entirely in permeable firn at holes B, C, and D; at drill hole E the brine was located entirely in ice. Station A (Fig. 7), located about 5 m from the shelf edge, included a pit excavated 2.5 m to sea level, which at this site coincided with the top of the saline ice of the brine zone. A hole was then cored approximately 6 m to the bottom of the shelf (Fig. 12). The core consisted of brine-infiltrated firn, now converted to saline ice. The bottom 1- to 2-cm section of core featured a dendritic crystal plate type structure, indicating that seawater was freezing onto the bottom at this location. The deepest hole, located at station F, 37 m beyond station 307, reached a depth of 59 m. Core data obtained from the 1977 and 1978 holes are listed in Tables 2–8.

Figure 12. Augering into saline snow ice of the brine zone at bottom of snow pit at station A.

Table 2. Data on firn from hole augered on high side of brine step at station 10, January 1977.

Measured				*Calculated*				
Depth (m)	*Temp. (°C)*	*Density (Mg/m³)*	*Melt salinity (‰)*	*Brine salinity (‰)*	*Brine vol. (‰)*	*Air vol. (‰)*	*Porosity (‰)*	*Density* (Mg/m³)*
17.15	−15	0.882	15.2	177	59.8	56.1	115.9	0.812
17.32	−15	0.892	13.0	177	51.7	43.1	94.8	0.832
17.47	−15	—	—	—	—	—	—	—
17.59	−14.75	0.900	12.2	175	50.1	33.7	83.8	0.842
17.82	—	0.894	16.0	175	64.5	44.1	108.6	0.819
18.0	—	0.878	14.0	175	63.4	61.2	124.6	0.804
18.10	—	—	—	—	—	—	—	—
18.21	—	0.883	15.5	174	62.5	55.4	117.9	0.811
18.35	—	0.896	16.0	174	65.4	42.0	107.4	0.820
18.50	—	0.883	12.6	174	51.4	52.4	103.8	0.822
18.65	—	—	—	—	—	—	—	—
18.73	−14.25	0.887	13.0	172	53.3	48.5	101.8	0.823

* Brine-free value.

Table 3. Data on firn from hole augered on low side of brine step at station 10b, January 1977.

Measured				*Calculated*				
Depth (m)	*Temp. (°C)*	*Density (Mg/m³)*	*Melt salinity (‰)*	*Brine salinity (‰)*	*Brine vol. (‰)*	*Air vol. (‰)*	*Porosity (‰)*	*Density* (Mg/m³)*
12.65	−16.75	0.613	—	—	—	—	—	—
12.80	−16.5	0.610	—	—	—	—	—	—
13.08	−16.5	0.613	—	—	—	—	—	—
13.15	−16.5	0.624	—	—	—	—	—	—
13.29	−16.5	0.614	—	—	—	—	—	—
13.45	−16.25	0.611	—	—	—	—	—	—
13.62	−16.25	0.627	—	—	—	—	—	—
13.87	—	0.638	—	—	—	—	—	—
14.18	−16	0.633	—	—				
14.30	—	0.639	—	—	—	—	—	—
14.45	—	0.631	—	—	—	—	—	—
14.58	—	0.652	—	—	—	—	—	—
14.80	—	0.648	—	—	—	—	—	—
15.07	−15.75	0.658	—	—	—	—	—	—
15.37	−15.5	0.644	—	—	—	—	—	—
15.64	—	0.662	—	—	—	—	—	—
15.87	−15.25	0.644	—	—	—	—	—	—
16.19	—	0.662	—	—	—	—	—	—
16.42	−15	0.664	—	—	—	—	—	—
16.79	−16.79	0.667	—	—	—	—	—	—
16.90	−15	0.657	—	—	—	—	—	—
17.10	—	0.666	—	—	—	—	—	—
17.30	—	0.663	—	—	—	—	—	—
17.50	−14.75	0.682	—	—	—	—	—	—
17.65	—	0.671	—	—	—	—	—	—
17.82	—	0.671	—	—	—	—	—	—
18.19	−14.5	0.669	—	—	—	—	—	—
18.46	—	0.696	—	—	—	—	—	—
18.73	−14.25	0.690	—	—	—	—	—	—
18.95	—	0.696	—	—	—	—	—	—
19.32	−14	0.697	—	—	—	—	—	—

Table 3 (cont'd).

	Measured			Calculated				
Depth (m)	*Temp. (°C)*	*Density (Mg/m³)*	*Melt salinity (‰)*	*Brine salinity (‰)*	*Brine vol. (‰)*	*Air vol. (‰)*	*Porosity (‰)*	*Density* (Mg/m³)*
19.38	—	—	—	—	—	—	—	—
19.65	—	0.711	—	—	—	—	—	—
19.86	−13.5	0.696	—	—	—	—	—	—
20.11	−13.5	0.694	—	—	—	—	—	—
20.40	—	0.704	—	—	—	—	—	—
20.76	−13.25	0.703	—	—	—	—	—	—
21.08	−13.25	0.714	—	—	—	—	—	—
21.45	−13	0.715	—	—	—	—	—	—
21.71	−13	0.727	—	—	—	—	—	—
21.80	—	0.714	—	—	—	—	—	—
21.95	—	—	—	—	—	—	—	—
22.10	—	0.800	15.0	162	68.1	144.0	214.1	0.732
22.17	−12.75	0.874	25.0	162	109.4	75.6	185.0	0.747
22.22	—	0.901	30.0	162	135.3	52.6	187.9	0.746
22.35	−12.75	0.903	30.0	162	135.6	50.5	186.1	0.748

* Brine-free value.

Table 4. Core data from station B, December 1978.

	Measured			Calculated				
Depth (m)	*Temp. (°C)*	*Density (Mg/m³)*	*Melt salinity (‰)*	*Brine salinity (‰)*	*Brine vol. (‰)*	*Air vol. (‰)*	*Porosity (‰)*	*Density* (Mg/m³)*
0.05	—	—	—	—	—	—	—	—
0.35	—	0.395	—	—	—	—	—	—
0.45	—	0.418	—	—	—	—	—	—
0.55	—	0.413	—	—	—	—	—	—
0.65	—	0.395	—	—	—	—	—	—
0.70	—	—	—	ice lens		—	—	—
0.75	—	0.403	—	—	—	—	—	—
0.85	—	0.439	—	—	—	—	—	—
0.90	−17.5	—	—	—	—	—	—	—
0.95	—	0.398	—	—	—	—	—	—
1.15	—	0.402	—	—	—	—	—	—
1.25	—	0.404	—	—	—	—	—	—
1.45	—	0.395	—	ice lens		—	—	—
1.65	—	0.377	—	—	—	—	—	—
1.75	−17.0	—	—	ice lens		—	—	—
1.85	—	0.392	—	—	—	—	—	—
1.95	—	0.393	—	—	—	—	—	—
2.05	—	—	—	1-cm-thick ice layer			—	—
2.15	—	0.432	—	—	—	—	—	—
2.25	—	0.411	—	—	—	—	—	—
2.45	—	0.390	—	—	—	—	—	—
2.55	−17.0	—	—	—	—	—	—	—
2.65	—	0.373	—	—	—	—	—	—
2.75	—	0.353	—	—	—	—	—	—
2.85	—	0.439	—	—	—	—	—	—
2.95	—	0.436	—	—	—	—	—	—
3.15	—	0.431	—	—	—	—	—	—
3.25	−17.2	—	—	—	—	—	—	—
3.35	—	0.448	—	—	—	—	—	—
3.45	—	0.466	—	—	—	—	—	—

Table 4 (cont'd). Core data from station B, December 1978.

	Measured			Calculated				
Depth (m)	Temp. (°C)	Density (Mg/m³)	Melt salinity (°/oo)	Brine salinity (°/oo)	Brine vol. (°/oo)	Air vol. (°/oo)	Porosity (°/oo)	Density* (Mg/m³)
3.65	—	0.513	—	—	—	—	—	—
3.75	—	0.514	—	—	—	—	—	—
3.85	−16.0	—	—	—	—	—	—	—
3.95	—	0.461	—	—	—	—	—	—
4.05	—	0.453	—	—	—	—	—	—
4.15	−15.4	0.458	—	—	—	—	—	—
4.25	—	0.475	—	—	—	—	—	—
4.35	—	0.513	—	—	—	—	—	—
4.40	—	0.488	—	—	—	—	—	—
4.55	—	0.498	—	—	—	—	—	—
4.65	—	0.483	—	—	—	—	—	—
4.75	—	0.502	—	—	—	—	—	—
4.85	—	0.518	—	—	—	—	—	—
4.95	—	0.509	—	—	—	—	—	—
5.05	—	0.539	—	—	—	—	—	—
5.15	−12.8	—	—	—	—	—	—	—
5.25	—	0.530	—	—	—	—	—	—
5.35	—	0.503	—	—	—	—	—	—
5.45	—	0.540	—	—	—	—	—	—
5.55	—	0.558	—	—	—	—	—	—
5.65	—	0.539	—	—		—	—	—
5.75	−11.4	—	—	—	—	—	—	—
5.85	—	0.550	—	—	—	—	—	—
6.05	—	0.535	—	—	—	—	—	—
6.15	—	0.542	—	—	—	—	—	—
6.25	—	0.527	—	—	—	—	—	—
6.35	—	0.528	—	—	—	—	—	—
6.45	−9.8	—	—	—	—	—	—	—
6.55	—	0.546	—	—	—	—	—	—
6.65	—	0.537	—	—	—	—	—	—
6.85	—	0.520	—	—	—	—	—	—
6.95	—	0.563	—	—	—	—	—	—
7.05	—	0.568	—	—	—	—	—	—
7.15	—	0.558	—	—	—	—	—	—
7.25	—	0.541	—	—	—	—	—	—
7.35	—	0.571	—	—	—	—	—	—
7.45	−7.3	—	—	—	—	—	—	—
7.55	—	0.568	—	—	—	—	—	—
7.65	—	0.561	—	—	—	—	—	—
7.75	—	0.612	—	—	—	—	—	—
7.85	−6	—	—	—	—	—	—	—
7.95	—	0.596	—	—	—	—	—	—
8.05	—	0.598	—	—	—	—	—	—
8.15	—	0.622	—	—	—	—	—	—
8.25	−5.4	—	—	—	—	—	—	—
8.35	—	0.593	—	—	—	—	—	—
8.48	—	—	—	ice lens		—	—	—
8.55	—	0.611	—	—	—	—	—	—
8.65	—	0.606	—	—	—	—	—	—
8.75	—	0.592	—	—	—	—	—	—
8.80	−3.7	—	—	—	—	—	—	—
8.85	−3.6	0.706	—	brine layer		—	—	—
9.00	—	0.831	6.9	62	84.0	106.5	190.5	0.743
9.10	—	0.877	8.2	62	105.3	59.5	164.8	0.766
9.20	−3.6	0.870	7.4	62	94.3	65.5	159.8	0.774
9.30	—	0.898	7.2	62	94.7	35.1	12[illegible].8	0.798
9.40	—	0.896	4.9	62	64.3	32.8	97.1	0.828
9.50	—	0.885	2.9	62	38.6	41.8	80.4	0.844
9.60	—	0.877	3.7	61	48.8	51.2	100.0	0.825

Table 4 (cont'd).

	Measured			*Calculated*				
Depth (m)	*Temp. (°C)*	*Density (Mg/m³)*	*Melt salinity (‰)*	*Brine salinity (‰)*	*Brine vol. (‰)*	*Air vol. (‰)*	*Porosity (‰)*	*Density* (Mg/m³)*
9.70	−3.5	0.864	—	61	—	—	—	—
9.80	—	0.882	2.2	61	29.2	42.9	72.1	0.851
9.90	—	0.882	3.0	61	39.8	44.4	84.2	0.840
10.00	—	0.870	3.0	61	39.6	48.8	88.4	0.836
10.10	—	0.871	2.5	61	33.2	55.4	88.6	0.836
10.20	—	0.884	3.1	60	41.8	42.5	84.3	0.840
10.30	—	0.889	3.1	60	42.0	37.1	79.1	0.845
10.40	—	0.889	—	—	—	—	—	—
10.50	−3.4	0.888	—	—	—	—	—	—

* Brine-free value.

Table 5. Core data from station C, December 1978.

	Measured			*Calculated*				
Depth (m)	*Temp. (°C)*	*Density (Mg/m³)*	*Melt salinity (‰)*	*Brine salinity (‰)*	*Brine vol. (‰)*	*Air vol. (‰)*	*Porosity (‰)*	*Density* (Mg/m³)*
1	—	—	—	—	—	—	—	—
2	—	0.440	—	—	—	—	—	—
3	—	0.440	—	—	—	—	—	—
4	—	0.494	—	—	—	—	—	—
5	—	0.474	—	—	—	—	—	—
6	—	0.488	—	—	—	—	—	—
7	—	0.501	—	—	—	—	—	—
8	—	0.556	—	—	—	—	—	—
9	—	0.550	—	—	—	—	—	—
10	—	0.592	—	—	—	—	—	—
11	—	0.602	—	—	—	—	—	—
12	—	0.613	—	—	—	—	—	—
13	—	0.620	—	—	—	—	—	—
14	—	0.632	—	—	—	—	—	—
15	—	0.652	—	—	—	—	—	—
16	—	0.664	—	—	—	—	—	—
16.95	—	—	—	ice lenses		—	—	—
17	—	0.664	—	—	—	—	—	—
18	—	0.680	—	—	—	—	—	—
19	—	0.695	—	—	—	—	—	—
19.45	—	—	—	brine layer		—	—	—
19.50	—	0.827	—	—	—	—	—	—
19.62	—	0.854	14.0	—	—	—	—	—
19.77	—	0.837	8.9	—	—	—	—	—
20.02	—	—	13.5	—	—	—	—	—
20.15	—	—	15.3	—	—	—	—	—
20.35	—	—	10.5	—	—	—	—	—
20.45	—	—	11.0	—	—	—	—	—
20.87	—	—	8.1	—	—	—	—	—

* Brine-free value.

Table 6. Core data from station D, December 1978.

Measured				*Calculated*				
Depth (m)	*Temp. (°C)*	*Density (Mg/m³)*	*Melt salinity (‰)*	*Brine salinity (‰)*	*Brine vol. (‰)*	*Air vol. (‰)*	*Porosity (‰)*	*Density* (Mg/m³)*
1	—	0.435	—	—	—	—	—	—
2	—	0.391	—	—	—	—	—	—
3	—	0.393	—	—	—	—	—	—
4	—	0.436	—	—	—	—	—	—
5	—	0.527	—	—	—	—	—	—
6	—	0.487	—	—	—	—	—	—
7	—	0.490	—	—	—	—	—	—
8	—	0.555	—	—	—	—	—	—
9	—	0.535	—	—	—	—	—	—
10	—	0.573	—	—	—	—	—	—
11	—	0.614	—	—	—	—	—	—
12	—	0.571	—	—	—	—	—	—
13	−21	0.586	—	—	—	—	—	—
14	—	0.607	—	—	—	—	—	—
15	—	0.625	—	—	—	—	—	—
16	—	0.648	—	—	—	—	—	—
17	—	0.654	—	—	—	—	—	—
18	—	0.671	—	—	—	—	—	—
19	—	0.662	—	—	—	—	—	—
20	—	0.668	—	—	—	—	—	—
21	—	0.684	—	—	—	—	—	—
22	−19	0.704	—	—	—	—	—	—
23	—	0.694	—	—	—	—	—	—
24	—	0.719	—	—	—	—	—	—
25	−18	0.701	—	—	—	—	—	—
26	—	0.718	—	—	—	—	—	—
27	—	0.740	—	—	—	—	—	—
28	−16.5	0.756	—	—	—	—	—	—
29	—	0.747	—	—	—	—	—	—
30	—	0.741	—	—	—	—	—	—
31	—	0.742	—	—	—	—	—	—
32	—	0.764	—	—	—	—	—	—
33	—	0.766	—	—	—	—	—	—
33.8	—	0.766	0.4	brine layer		—	—	—
33.92	—	0.781	—	—	—	—	—	—
34.08	—	0.818	1.8	177	6.6	111.7	118.3	0.810
34.26	—	0.824	4.4	177	16.2	107.7	123.9	0.805
34.46	−15	0.848	5.3	177	20.0	82.6	102.7	0.825
34.61	—	0.868	13.1	177	50.7	68.9	119.6	0.809
34.77	—	0.892	14.6	177	58.1	44.8	102.9	0.824
34.92	—	0.876	8.1	177	31.6	55.2	86.8	0.839
35.10	—	0.856	10.8	177	41.2	79.5	120.7	0.808
35.27	—	—	13.4	—	—	—	—	—
35.99	—	—	9.5	—	—	—	—	—
36.6	—	—	11.0	—	—	—	—	—

* Brine-free value.

Table 7. Core data from station E, December 1978.

Measured				*Calculated*				
Depth (m)	*Temp. (°C)*	*Density (Mg/m³)*	*Melt salinity (‰)*	*Brine salinity (‰)*	*Brine vol. (‰)*	*Air vol. (‰)*	*Porosity (‰)*	*Density* (Mg/m³)*
1	—	0.396	—	—	—	—	—	—
2	—	0.430	—	—	—	—	—	—
3	—	0.424	—	—	—	—	—	—
4	—	0.450	—	—	—	—	—	—
4.24	—	—	—	ice layer		—	—	—
5	—	0.505	—	—	—	—	—	—
6	—	0.518	—	—	—	—	—	—
7	—	0.513	—	—	—	—	—	—
9	—	0.528	—	—	—	—	—	—
9	—	0.575	—	ice layer		—	—	—
10	—	0.568	—	—	—	—	—	—
11	—	0.577	—	—	—	—	—	—
12	—	0.587	—	—	—	—	—	—
12.3	—	—	—	ice layer		—	—	—
13	—	0.609	—	—	—	—	—	—
14	—	0.615	—	—	—	—	—	—
15	—	0.623	—	—	—	—	—	—
16	—	—	—	—	—	—	—	—
17	—	0.638	—	—	—	—	—	—
18	—	0.637	—	—	—	—	—	—
19	—	0.649	—	—	—	—	—	—
20	—	0.668	—	—	—	—	—	—
21	—	0.660	—	—	—	—	—	—
22	—	0.691	—	—	—	—	—	—
23	—	0.699	—	—	—	—	—	—
24	—	0.709	—	—	—	—	—	—
25	—	0.704	—	—	—	—	—	—
26	—	0.719	—	—	—	—	—	—
27	—	0.713	—	—	—	—	—	—
27.23	—	—	—	ice layer		—	—	—
28	—	0.731	—	ice layer		—	—	—
28.73	—	—	—	½ cm ice layer		—	—	—
29	—	0.729	—	—	—	—	—	—
30	—	0.754	—	—	—	—	—	—
31	—	0.736	—	—	—	—	—	—
32	—	0.758	—	—	—	—	—	—
33	—	0.759	—	—	—	—	—	—
34	—	0.770	—	—	—	—	—	—
35	—	0.778	—	—	—	—	—	—
36	—	0.755	—	—	—	—	—	—
37	—	0.798	—	—	—	—	—	—
38	—	0.767	—	—	—	—	—	—
39	—	0.791	—	—	—	—	—	—
40	—	0.811	—	—	—	—	—	—
40.7	—	—	—	4-cm-thick fine-grained ice band				—
41	—	0.802	—	—	—	—	—	—
42	—	0.808	—	—	—	—	—	—
43	—	0.798	—	—	—	—	—	—
44	—	0.832	—	—	—	—	—	—
45	—	0.836	—	—	—	—	—	—
46	—	0.826	—	—	—	—	—	—
47	—	0.827	—	—	—	—	—	—
48	—	0.834	—	—	—	—	—	—
49	—	0.847	—	—	—	—	—	—
50	—	0.851	—	—	—	—	—	—

Table 7 (cont'd). Core data from station E, December 1978.

	Measured			Calculated				
Depth (m)	*Temp. (°C)*	*Density (Mg/m³)*	*Melt salinity (‰)*	*Brine salinity (‰)*	*Brine vol. (‰)*	*Air vol. (‰)*	*Porosity (‰)*	*Density* (Mg/m³)*
50.37	—	—	—	brine in core		—	—	—
50.5	—	0.855	2.0	186	7.2	71.9	79.1	0.847
50.6	—	0.866	1.3	186	4.7	59.3	64.0	0.860
50.7	—	0.869	3.0	186	11.0	57.7	68.7	0.856
50.8	—	0.867	2.2	186	8.0	59.1	67.1	0.857
50.9	—	0.865	1.0	186	3.6	60.0	63.6	0.860
51	—	0.855	—	186	—	—	—	—
51.1	—	—	10.1	186	—	—	—	—
51.2	—	—	7.0	186	—	—	—	—
51.34	—	0.898	9.2	186	34.7	32.6	67.3	0.857
51.40	−16.3	0.865	2.7	186	9.8	61.7	71.5	0.854
51.55	—	—	2.2	186	—	—	—	—
51.65	—	0.893	15.0	186	56.3	44.0	100.3	0.827
51.75	—	0.870	4.1	186	15.0	57.7	72.7	0.852
51.88	—	0.867	1.4	186	5.1	58.3	63.4	0.861
52.00	—	—	9.6	—	—	—	—	—
52.11	—	—	14.6	—	—	—	—	—
52.20	—	—	0.2	—	—	—	—	—
52.30	—	—	2.1	—	—	—	—	—
52.40	—	—	—	—	—	—	—	—
52.48	—	—	3.2	—	—	—	—	—

* Brine-free value.

Table 8. Core data from station F, December 1978.

Depth (m)	*Density (Mg/m³)*	*Stratigraphic observations*	*Depth (m)*	*Density (Mg/m³)*	*Stratigraphic observations*
1.25	0.400		13.40	0.607	
2.85	0.440		13.75	0.607	
3.20	0.444		14.45	0.611	
3.53	—	3- to 4-mm-thick ice layer	14.80	—	4-mm ice layer
3.80	0.482		15.30	0.628	
3.95	—	ice chunks	15.95	0.627	
4.15	—	1-cm-thick ice layer	16.60	0.625	
4.40	0.480		17.15	0.636	
5.25	0.485		17.60	—	2-cm-thick zone of scattered ice pellets
5.75	0.490		17.65	0.653	
6.45	0.531		18.55	—	10-cm-thick diffuse dirt zone
7.00	0.521		18.65	0.663	
7.40	0.540		19.40	0.655	
8.00	0.544		19.70	—	ice lens
8.40	0.548		19.95	—	5-cm zone of ice lenses
8.95	0.548		20.00	0.659	
9.10	0.556		20.15	0.676	
9.40	0.566		20.40	0.662	
10.05	0.587		21.60	0.681	
10.50	0.564		22.40	0.670	
10.90	0.586		23.15	0.687	
11.70	0.590		23.70	0.686	
12.41	—	5-mm-thick ice layer	24.40	0.709	
12.45	0.581		25.15	0.704	
13.22	—	thin ice lens	25.60	0.706	
13.33	—	½-cm ice layer	26.50	0.711	

Table 8 (cont'd).

Depth (m)	*Density (Mg/m³)*	*Stratigraphic observations*
26.87	—	1-cm-thick ice layer
27.15	0.726*	
27.80	0.721	
28.55	0.724	
29.65	—	thin ice lenses between 29.65 and 30.00 m
29.70	0.737	
30.15	0.736	
30.70	0.757	
31.40	0.753	
32.75	—	thin ice lens
33.20	0.754	
34.40	0.774	
34.95	0.783	
35.40	0.773	
36.00	—	2- to 3-cm-thick dirty layer
36.55	0.780	
37.05	—	5-mm-thick ice layer
37.40	—	4-mm-thick ice layer
37.50	—	5-mm-thick ice layer
37.90	0.794	
38.00	—	thin ice lens
38.30	—	from this depth on much of the core showed a good banded structure consisting of fine- and coarser-grained material
39.15	0.782	
40.05	0.795	
40.55	0.823	
42.40	0.816	
42.60	0.815	
43.40	0.832	
44.40	0.829	
45.60	0.826	3-mm-thick ice layer
46.40	0.831	
47.60	0.834	
49.70	0.842	
50.20	0.853	
50.40	0.846	
51.20	0.856	
51.95	0.850	
52.40	0.856	
53.20	0.850	
54.00	—	1-mm-thick ice lens
54.95	0.858	
55.40	0.884	
56.60	0.874	
57.40	0.874	
58.40	0.873	
59.40	0.865	minimum density value—thin slab missing from side of core

Density and temperature profiles

The depth-density profiles for the firn at various drill sites are shown in Figures 13-18, and the temperature versus depth profiles obtained at stations B, 10b and D are shown graphically in Figure 19. Extrapolating the temperature profiles in Figure 19 to a temperature of -1.8°C, the freezing point of the seawater, would yield apparent shelf thicknesses of 25.5 m at station B, 49.5 m at station 10b, and 80 m at station D. The thickness values for stations B and 10b agree very well with the values of ice shelf thickness that can be obtained from Figure 7. The value for station D is about 9 m less than the indicated depth in Figure 7. This suggests that the temperature gradient becomes steeper with depth at this location, and since there is no bottom shear the change must be due to a change in density.

Curves obtained by least squares analysis of the depth-density data obtained at drilling stations B, C, D, E and F are shown collectively in Figure 20. Each curve represents the firn depth-density trend down to the top of the brine layer except at station F, where no brine was encountered. These curves, together with the temperature profiles in Figure 19, reveal that as one moves further inland on the ice shelf the thermal and density regimes of the firn change. In short, at a depth of 10 m at station B the snow is much warmer and denser than at succeeding stations further inland. This is due to more rapid heat transfer through the thinner part of a wedge-shaped ice shelf. Where the ice shelf is thin more heat escapes to the atmosphere from the underlying seawater and larger seasonal temperature variations occur within the firn. These effects, in conjunction with lower rates of snow accumulation, accelerate the densification process in the firn as one moves toward the ice front.

Ice shelf freeboard

From the data listed in Table 1 we can calculate the effective bulk density of the ice shelf (ϱ_a) at station 24 from

$$\varrho_a = \left(1 - \frac{F}{D_T}\right)\varrho_w \tag{5}$$

where F = freeboard
ϱ_w = density of seawater (~ 1.0275 Mg/m³)
D_T = total ice shelf thickness.

Given that the surface elevation is 25 m and the keel depth K is 88 m, then D_T = 113 m, and from eq 5, ϱ_a is 0.800 Mg/m³.

From the values listed in Table 1, the shelf-

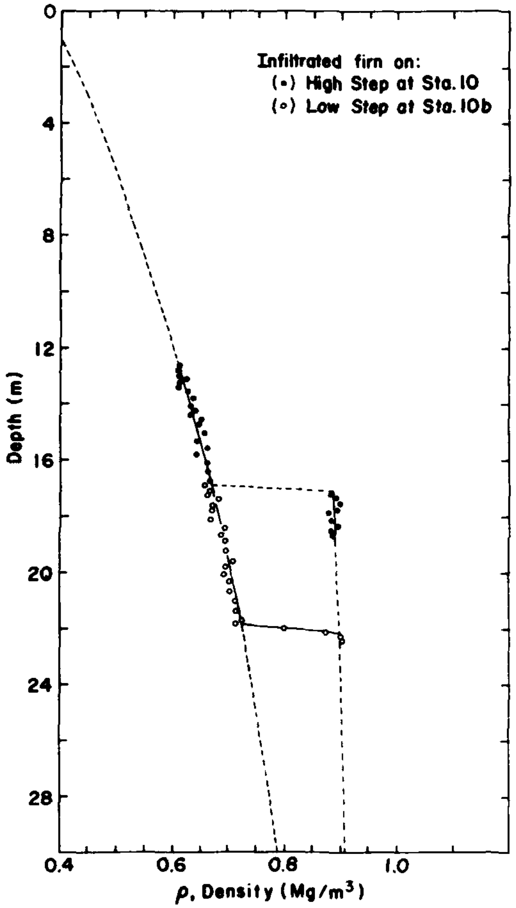

Figure 13. Depth–density profiles at stations 10 and 10b. The abrupt increase in the density shown at the bottom of each station hole marks the firn–saline ice transition.

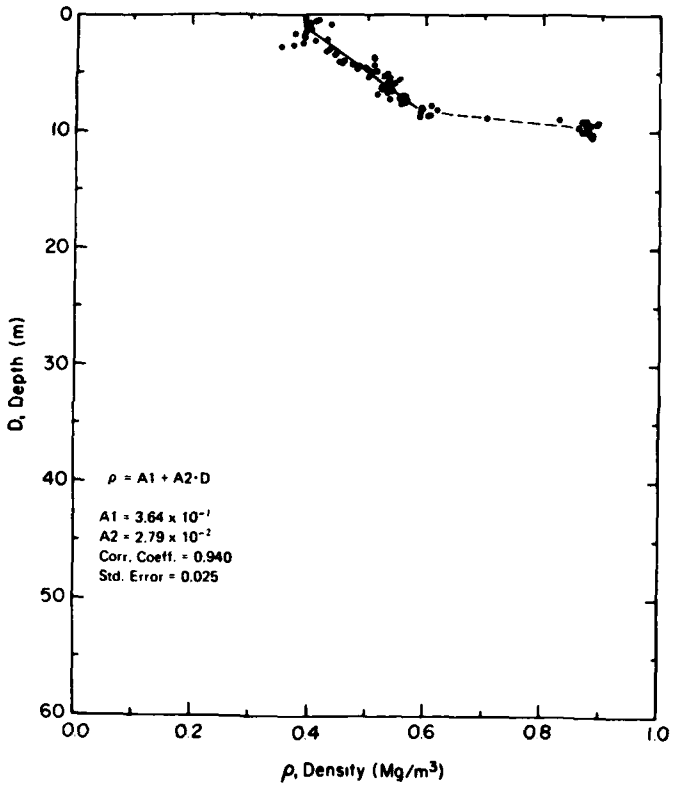

Figure 14. Depth–density profile at station B. The sudden increase in density marks the firn–saline ice transition.

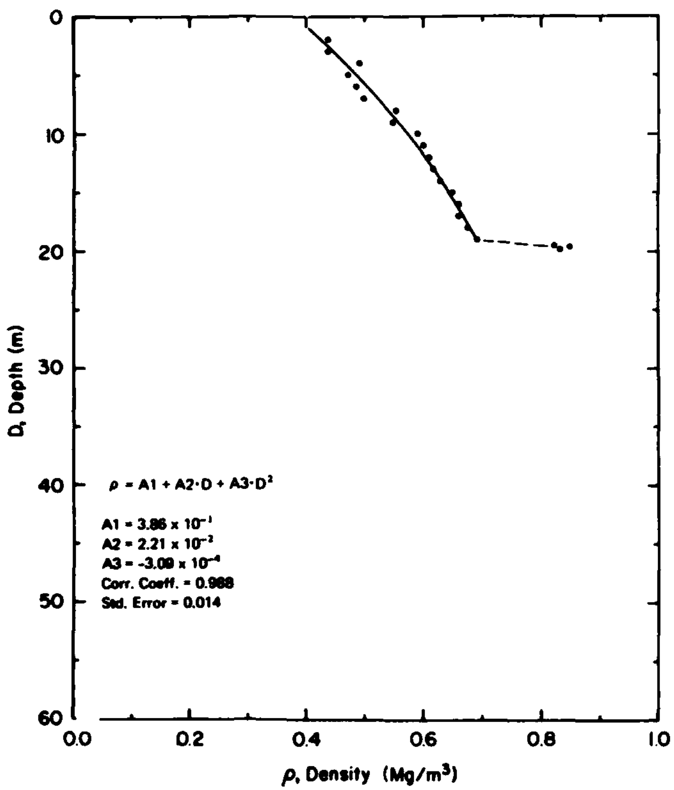

Figure 15. Depth–density profile at station C. The sudden increase in density marks the firn–saline ice transition.

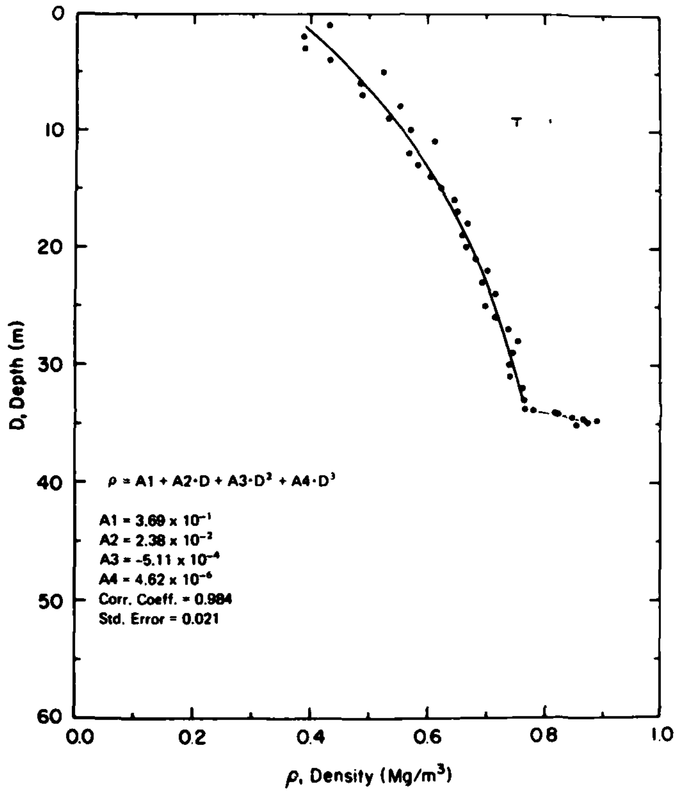

Figure 16. Depth–density profile at station D. The sudden increasee in density marks the firn–saline transition.

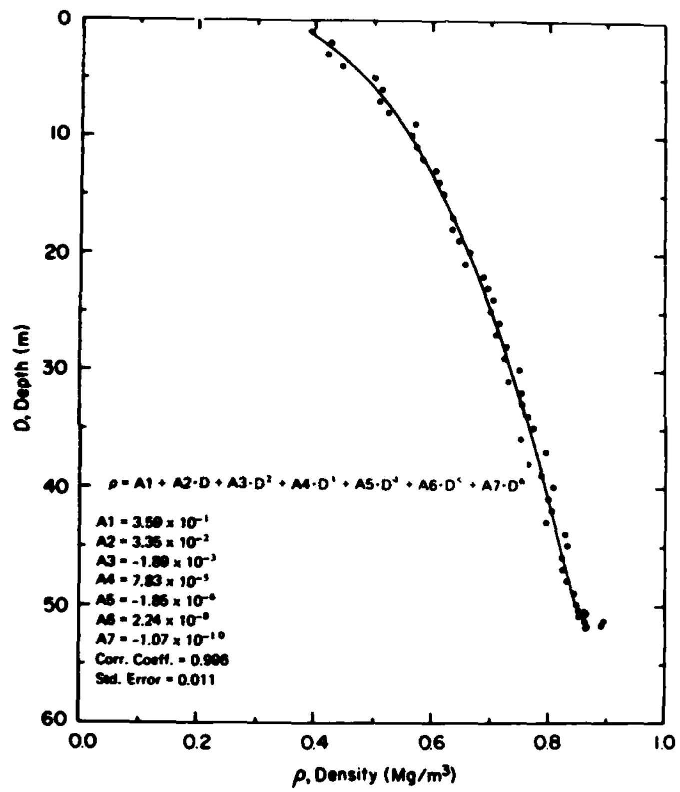

Figure 17. Depth–density profile at station E. The sudden increase in density marks the firn–saline ice transition.

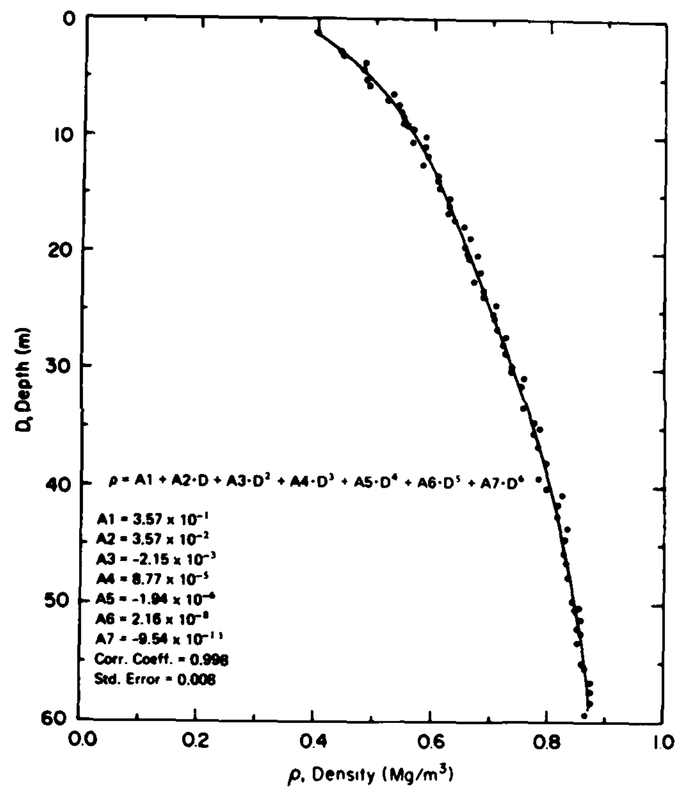

Figure 18. Depth–density profile at station F. The sudden increase in density marks the firn–saline ice transition.

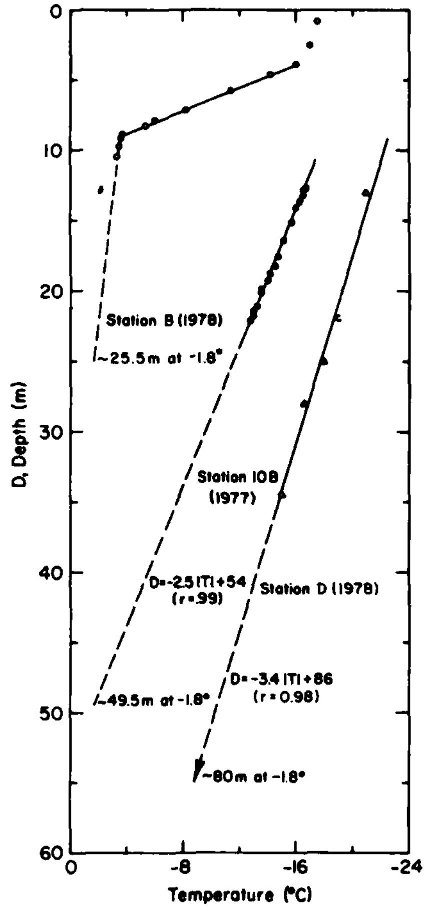

Figure 19. Depth–temperature profiles for stations B, 10b and D.

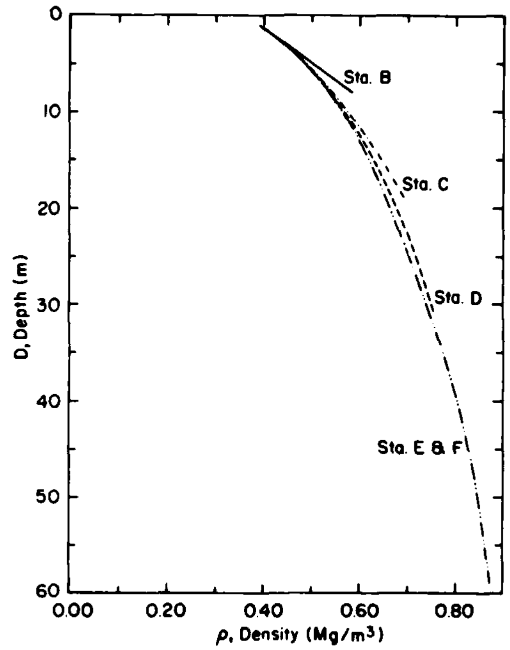

Figure 20. Depth–density profiles in brine-free firn at the five stations (B–F) located along the main ice shelf traverse line.

thickness-to-freeboard ratio is found to be ~4.5:1. This is somewhat higher than the ~4.15:1 ratio that would be derived from Gow's (1963) relationship based on density data from the 258-m-thick Ross Ice Shelf at Little America V. The higher value for station 24 is believed due to brine loading and higher firn densities deflecting the ice shelf downward. A deflection due to brine loading was quite evident in our 1977 elevation survey, which showed a marked change in slope near station 10 (see insert A′, Fig. 7). This change in slope occurred over such a short distance that it was first observed visually and subsequently verified by the elevation survey data.

Brine upwelling

Another interesting finding from the January 1981 radio echo resurvey was the observation that brine had risen 8.7 m inside the 0.15-m-diameter borehole at station E and 0.5 m in the borehole at station D. At station D, the hole bottom had 0.7 m of hoarfrost underlain by a firm surface slightly moistened with brine. At station E, the radio echo data (Fig. 21) revealed at least two horizons where the brine had migrated laterally away from the hole. At the 8.7-m upwell level, the brine had moved 2 to 3 m laterally, while at the mid-upwell level it had moved outward approximately 5 m. It is not known whether the 8.7-m upwelling represents the maximum hydraulic head in the brine layer at station E, as upwelling may have been arrested by liquid freezing under the lower temperatures at the higher elevation. Lead line sounding indicated a "hard bottom" existed at station E.

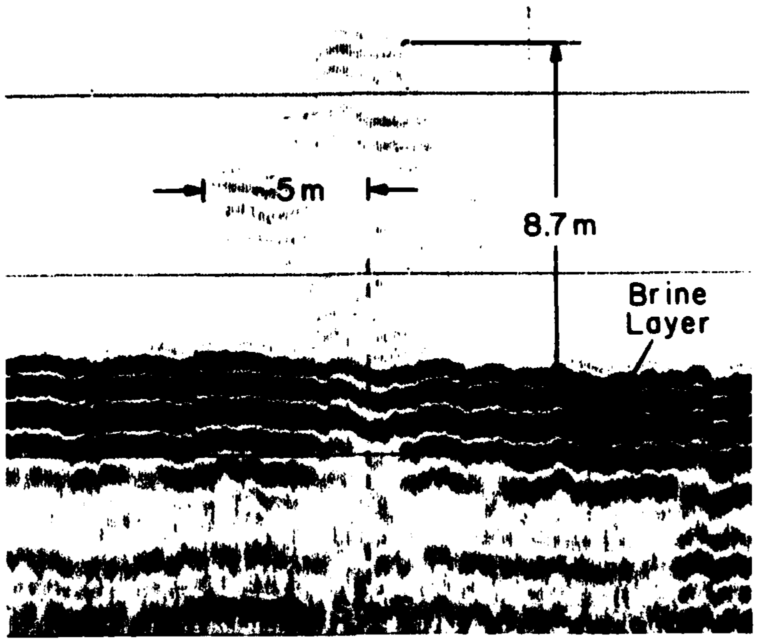

Figure 21. Radio echo profile in vicinity of drilling station E showing signature of brine upwelling and lateral migration measured 26 months after hole was drilled.

Brine chemistry

Chemical analysis of brine-infiltrated cores from several drill holes along the main profile shows that freeze-fractionation of the seawater as it penetrates the ice shelf preferentially precipitates virtually all sodium sulfate (mirabilite) before the inland boundary of brine penetration is reached. For example, in samples from near the nose of the 4.4-m-high brine wave (on the high side of the step) the sulfate-to-sodium ratios are essentially the same as for seawater (0.25), or higher (0.59) where sodium sulfate has precipitated locally. However, this ratio decreases 4-fold to 0.08 immediately beyond the brine wave (on the low side of the step) in samples from an earlier infiltrated zone across which the new brine wave is known to be migrating. Near the terminal boundary of brine infiltration, the sulfate-to-sodium ratio is reduced to 0.028, which is an order of magnitude less than the seawater value. These data confirm the results obtained earlier by Wilson and Heine (1964). Concomitant removal of water by freezing within the pore spaces of the firn grains has produced brines with a salinity approximately six times more concentrated (S = 186‰) than the original seawater (S = 33‰). We present a more detailed discussion of the brine chemistry and its glaciological implications in another report (Cragin et al. 1982).

CONCLUSIONS

Observations of a 4.4-m-high brine step in the McMurdo Ice Shelf show that it has migrated about 1.2 km since it was first discovered in January 1977 and resurveyed in January 1981. The present wave is overriding an older brine-soaked layer. This migration is proof of the dynamic nature of the step, which the evidence indicates represents the leading edge of a brine wave that originated at the ice front during a recent major break-out of the McMurdo Ice Shelf. The inland boundary of brine penetration, located 8 to 10 km from the ice front, is characterized by a series of descending steps that are also interpreted as representing the present terminal positions of several separate intrusions of brine similar in origin to the 4.4-m brine step. The location of the inland boundary of brine percolation is probably controlled to a large extent by the depth at which brine encounters the firn/ice transition (≈43-m depth). However, this boundary is not entirely fixed by firn permeability considerations alone, since a small but measurable movement of brine is still occurring in ice at the inland boundary. This continued migration of brine is attributed partially to dissolution of the surrounding ice by the concentrated brine as it moves into deeper and warmer parts of the ice shelf. Freeze-fractionation of the seawater as it percolates through the ice shelf preferentially precipitates virtually all sodium sulfate by the time the brine reaches the inland boundary. Concomitant removal of water by freezing in the pore spaces of the infiltrated firn produces residual brines approximately six times more concentrated that the original seawater. This brine is retained in the ice in the form of liquid-filled vesicles. We conclude that lateral infiltration is the principal mechanism of brine soaking of firn in the McMurdo Ice Shelf, and that the overall process is dominated by wave-like intrusions of seawater triggered by periodic break-outs of the ice front in McMurdo Sound.

LITERATURE CITED

Clough, J.W. (1973) Radio echo sounding: brine percolation layer. *Journal of Glaciology,* **2**(64): 141-143.

Clough, J.W. and C.R. Bentley (1967) Electromagnetic sounding of glacial and shelf ice. *Antarctic Journal of the United States,* **2**(4): 119-120.

Cragin, J.H., A.J. Gow and A. Kovacs (1982) Chemical fractionation of brine in the McMurdo Ice Shelf. U.S. Army Cold Regions Research and Engineering Laboratory, CRREL Report (in preparation).

Dubrovin, L.I. (1962) O rassolakh v shel'fovykh lednikakh. *Inform. Byull. Sov. Antarkt. Eksped.,* **35**: 35-38.

Eide, I.E. and S. Martin (1975) The formation of brine drainage features in young sea ice. *Journal of Glaciology,* **14**(70): 137-154.

Gow, A.J. (1963) Deep core studies of the accumulation and densification of snow at Byrd Station and Little America V, Antarctica. CRREL Research Report 197, 45 pp. AD-669240.

Heine, A.J. (1963) Ice breakout around the southern end of Ross Island, Antarctica. *New Zealand Journal of Geology and Geophysics,* **6**(3): 395-402.

Heine, A.J. (1967) The McMurdo Ice Shelf, Antarctica, a preliminary report. *New Zealand Journal of Geology and Geophysics,* **10**(2): 474-478.

Heine, A.J. (1968) Brine in the McMurdo Ice Shelf, Antarctica. *New Zealand Journal of Geology and Geophysics,* **11**(4): 829-839.

Hoekstra, P., T.E. Osterkamp and W.F. Weeks (1965) Migration of liquid inclusions in single ice crystals. *Journal of Geophysical Research,* **70**: 5035-5041.

Hoffman, C.R. (1974) Engineering manual for McMurdo Station. Naval Civil Engineering Laboratory, revised 1979, 536 pp.

Kovacs, A. and A.J. Gow (1975) Brine infiltration in the McMurdo Ice Shelf, McMurdo Sound, Antarctica. *Journal of Geophysical Research,* **80**(15): 1957-1961.

Kovacs, A. and A.J. Gow (1977a) Dielectric constant and reflection coefficient of the snow and near-surface internal layers in the McMurdo Ice Shelf. *Antarctic Journal of the United States,* **12**(4): 137-138.

Kovacs, A. and A.J. Gow (1977b) Subsurface measurements of the Ross Ice Shelf, McMurdo Sound, Antarctica. *Antarctic Journal of the United States,* **12**(4): 146-148.

Kovacs, A. and R.M. Morey (1979) Remote detection of massive ice in permafrost along the Alyeska Pipeline and the pump station feeder gas pipeline. In *Proceedings of the Specialty Conference on Pipelines in Adverse Environments, ASCE, New Orleans, Louisiana,* pp. 268-279.

Nye, J.F. and F.C. Frank (1973) Hydrology of the intergranular veins in a temperate glacier. In *Symposium on the Hydrology of Glaciers, Cambridge, England, 7-13 September 1969.* Glaciological Society, Publication No. 95, pp. 157-161.

Paige, R.A. (1969) Bottom melting of the McMurdo Ice Shelf, Antarctica. *Journal of Glaciology,* **8**(52): 170-171.

Paige, R.A. (1971) Breakout of the McMurdo Ice Shelf. Naval Civil Engineering Laboratory, Internal Report 7.

Rand, J.H. (1976) The USACRREL shallow drill. In *Ice-Core Drilling* (J.F. Splettstoesser, Ed.). The University of Nebraska Press.

Raymond, C.F. and W.D. Harrison (1975) Some observations on the behavior of liquid and gas phases in temperate glacier ice. *Journal of Glaciology,* **14**(71): 213-233.

Risk, G.F. and M.P. Hochstein (1967) Subsurface measurements of the McMurdo Ice Shelf, Antarctica. *New Zealand Journal of Geology and Geophysics,* **10**(2): 484-497.

Seidensticker, R.G. (1966) Letter to the editor. *Journal of Geophysical Research,* **71**: 2180-2181.

Shimizu, H. (1970) Air permeability of deposited snow. *Contributions from the Institute of Low Temperature Science, Hokkaido University,* Ser. A, No. 22.

Smith, B.M. and S. Evans (1972) Radio echo sounding: Absorption and scattering by water inclusions and ice lenses. *Journal of Glaciology,* **11**(61): 133-146.

Stewart, M.K. (1975) Hydrogen and oxygen isotope studies on the McMurdo Ice Shelf, Antarctica. *New Zealand Journal of Geology and Geophysics,* **18**(1): 49-64.

Stuart, A.W. and C. Bull (1963) Glaciological observations on the Ross Ice Shelf near Scott Base, Antarctica. *Journal of Glaciology,* **4**(34): 399–414.

Thomas, R.H. (1973) The dynamics of the Brunt Ice Shelf, Coats Land, Antarctica. British Antarctic Survey Scientific Report, No. 79, pp. 125–136.

Thomas, R.H. (1975) Liquid brine in ice shelves. *Journal of Glaciology,* **14**(70): 125–136.

Wilson, A.T. and A.J. Heine (1964) The chemistry of ice shelf brines. *Journal of Glaciology,* **5**(38): 265–267.

A facsimile catalog card in Library of Congress MARC format is reproduced below.

Kovacs, A.
The brine zone in the McMurdo Ice Shelf, Antarctica / by A. Kovacs, A.J. Gow, J.H. Cragin and R.M. Morey. Hanover, N.H.: Cold Regions Research and Engineering Laboratory; Springfield, Va.: available from National Technical Information Service, 1982.
v, 35 p., illus.; 28 cm. (CRREL Report 82-39.)
Prepared for National Science Foundation by Corps of Engineers, U.S. Army Cold Regions Research and Engineering Laboratory.
Bibliography: p. 27.
1. Antarctica. 2. Brines. 3. Firn. 4. Glaciers. 5. Ice shelves. 6. Radio echo sounding. I. Gow, A.J. II. Cragin, J.H. III. Morey, R.M. IV. United States. Army. Corps of Engineers. V. Cold Regions Research and Engineering Laboratory, Hanover, N.H. VI. Series: CRREL Report 82-39.